Research Square

Preprints are preliminary reports that have not undergone peer review.
They should not be considered conclusive, used to inform clinical practice,
or referenced by the media as validated information.

HDAC1 overexpression reduces chemosensitivity by promoting cell survival and inhibiting apoptotic responses in Luminal A breast cancer cells

Yuqian Hu
Tianjin Fourth Central Hospital
Tingting Lyu
Chinese Academy of Medical Sciences & Peking Union Medical CollegeChinese Academy of Medical Sciences
Xianyun Ji
Shanxi Medical University
Jing Gao
Tianjin Fourth Central Hospital
Zhaoyan Qiang
Tianjin Medical University
Jianhong Zhang
Zhang_jianhong66@sina.com

Tianjin Fourth Central Hospital

Article

Keywords: HDAC1, Luminal A breast cancer, chemosensitivity, apoptosis, epigenetic regulation

Posted Date: October 26th, 2026

DOI: https://doi.org/10.21203/rs.3.rs-11169296/v1

License: This work is licensed under a Creative Commons Attribution 4.0 International License.
Read Full License

Additional Declarations: No competing interests reported.

HDAC1 overexpression reduces chemosensitivity by promoting cell survival and inhibiting apoptotic responses in Luminal A breast cancer cells

Yuqian Hu [1], Tingting Lyu [2, #], Xianyun Ji [3], Jing Gao [1], Zhaoyan Qiang [4, *] and Jianhong Zhang [1, *].

[1] Pharmacy Department, Tianjin Fourth Central Hospital, No. 3 Zhongshan Road, Hebei District, Tianjin 300143, China.

[2] Chinese Academy of Medical Sciences, Peking Union Medical College, No. 9 Dongdan Santiao, Dongcheng District, Beijing 100730, China.

[3] Department of Pediatrics, Shanxi Medical University, Yingze Campus, No. 56 Xinjian South Road, Yingze District, Taiyuan City, Shanxi Province, 030001, China.

[4] Department of Pharmacology, College of Basic Medical, Tianjin Medical University, No. 22 Qixiangtai Road, Heping District, Tianjin, 300070, China.

[#]Yuqian Hu and Tingting Lyu should be considered joint first author.

*Correspondence authors. Emails:

Professor Jianhong Zhang: Zhang_jianhong66@sina.com

Professor Zhaoyan Qiang: qzyss1@163.com

Contributing authors: huyuqian0622@126.com; lvtingting1224@163.com; jixianyun2022@163.com; 1030412407@qq.com

Abstract

Background: Histone deacetylase 1 (HDAC1) is an important epigenetic regulator involved in tumor progression. However, whether HDAC1 overexpression reduces chemotherapy sensitivity in breast cancer by promoting cell survival and inhibiting apoptosis remains unclear.

Methods: In this study, we combined integrative bioinformatic analyses with experimental validation to investigate the role of HDAC1 in regulating chemosensitivity in breast cancer. HDAC1 expression patterns and prognostic significance were analyzed using genomic datasets. Gene signatures associated with chemosensitivity were identified across multiple independent cohorts, followed by functional enrichment and protein–protein interaction network analyses. Protein–protein docking and molecular dynamics simulations were performed to characterize the potential interaction between HDAC1 and YY1. Tumor microenvironment and immune checkpoint correlations were

also examined. Further, a stable HDAC1-overexpressing MCF-7 breast cancer cell line was generated using lentiviral transduction, and cellular responses to pirarubicin (THP), teniposide (VM-26), and cisplatin (DDP) were assessed using cell viability assays, morphological analysis, and flow cytometric apoptosis profiling.

Results: HDAC1 was significantly upregulated in breast cancer, especially in subtypes characterized by more aggressive biological features, and correlated with poor prognosis. HDAC1 overexpression in MCF-7 cells reduced chemosensitivity to THP, VM-26, and DDP, while significantly enhancing cell survival and reducing drug-induced apoptosis. HDAC1 was associated with key proteins involved in chemotherapy response and enriched in chromatin modification, p53/RB1, and NRF2-related pathways. Structural modeling further supported a potential HDAC1–YY1 interaction, suggesting a role for HDAC1 in reduced chemosensitivity in breast cancer. HDAC1 expression was closely associated with tumor microenvironment remodeling and immune checkpoint regulation in breast cancer.

Conclusion: In Luminal A breast cancer, HDAC1 overexpression reduces chemosensitivity by promoting cell survival and inhibiting apoptosis. HDAC1 may reduce chemosensitivity through coordinated regulation of chromatin remodeling and chemotherapy response-associated signaling pathways, including p53/RB1 and NRF2, potentially involving YY1. Targeting HDAC1 may represent a promising therapeutic strategy for restoring chemosensitivity.

Keywords: HDAC1; Luminal A breast cancer; chemosensitivity; apoptosis; epigenetic regulation

Introduction

Breast cancer (BRCA) is the most frequently diagnosed malignancy among women worldwide and continues to represent a major cause of cancer-related mortality. According to global cancer statistics, BRCA accounted for ~11.6% of newly diagnosed cancer cases (approximately 2.3 million) and 6.9% of cancer deaths (approximately 665,684) in 2022[1]. Luminal A breast cancer, the most common molecular subtype, is characterized by hormone receptor positivity, HER2 negativity, and relatively low proliferative activity[2]. Although endocrine therapy is the main systemic treatment for Luminal A tumors, chemotherapy remains an important option for selected patients, particularly those with high-risk disease, and its clinical benefit may be limited by reduced responsiveness to cytotoxic agents[3]. However, the clinical efficacy of

chemotherapy is frequently undermined by intrinsic or acquired reductions in chemosensitivity, which constitute major barriers to durable therapeutic responses and long-term survival[4]. Elucidating the molecular mechanisms underlying impaired chemosensitivity is therefore critical for developing more effective therapeutic strategies for breast cancer.

Epigenetic alterations have been increasingly recognized as important contributors to cancer development and therapy resistance [5]. Histone deacetylases (HDACs) are key regulators of chromatin organization and gene transcription, primarily through the removal of acetyl groups from histone and non-histone proteins [6]. Among these enzymes, histone deacetylase 1 (HDAC1), a member of the class I HDAC family, has attracted considerable attention because of involvement in multiple oncogenic processes [7,8]. In breast cancer, aberrant HDAC1 expression has been associated with aggressive tumor characteristics, including enhanced proliferation, invasive capacity and metastatic potential [9,10]. Clinical studies have further indicated that elevated HDAC1 levels correlate with higher tumor grade, increased proliferative activity and unfavorable prognosis [11].

Accumulating evidence indicates that HDAC1 regulates multiple biological processes associated with reduced chemosensitivity, including cell-cycle control, DNA damage repair, apoptosis, and epithelial–mesenchymal transition[12-15]. HDAC1 has also been reported to interact with major tumor suppressor proteins such as TP53 and RB1, both of which play critical roles in determining cellular sensitivity to anticancer therapies [16,17]. Histone deacetylase inhibitors (HDACis) exert antitumor effects by reversing histone deacetylation and inducing cell-cycle arrest, apoptosis, immune activation, anti-angiogenic responses, and defective DNA repair, and have demonstrated promising therapeutic efficacy across a broad spectrum of solid tumors and hematologic malignancies [18-20]. Moreover, HDAC1 contributes to reduced chemosensitivity through epigenetic regulation of chromatin accessibility and gene transcription, including modulation of promoters, enhancers, super-enhancers, and non-histone substrates [21]. However, the precise role of HDAC1 overexpression in regulating chemosensitivity and tumor cell survival remains incompletely defined.

In this study, we systematically elucidated the role of HDAC1 in breast cancer chemosensitivity through integrated multi-omics analyses of The Cancer Genome Atlas (TCGA), Clinical Proteomic Tumor Analysis Consortium (CPTAC), and Gene Expression Omnibus (GEO) datasets combined with in vitro functional assays. HDAC1

was markedly upregulated in breast cancer tissues, with elevated expression correlating with advanced clinical stage, adverse prognosis, and reduced chemosensitivity across molecular subtypes. We further established and validated a stable HDAC1-overexpressing MCF-7 cell model, in which HDAC1 overexpression conferred resistance to pirarubicin, teniposide, and cisplatin. HDAC1 overexpression was accompanied by increased cell viability and reduced drug-induced apoptosis, as consistently validated by cell viability assays, Hoechst 33258/PI staining, and Annexin V/PI flow cytometric analysis. Using GEO datasets, we identified 391 drug sensitivity-associated differentially expressed genes (DEGs), with functional enrichment analyses revealing preferential enrichment of HDAC1 in pathways governing resistance to cell death and apoptotic regulation. Construction of an HDAC1-centered protein–protein interaction (PPI) network revealed interactions between HDAC1 and key regulators, including TP53 and RB1. Protein–protein docking further predicted a favorable interaction between HDAC1 and YY1, while molecular dynamics simulations supported the structural stability of the predicted HDAC1–YY1 complex. Elevated HDAC1 expression was closely associated with altered chromatin modification states, p53/RB1 pathway dysfunction, and activation of the NRF2 pathway. Collectively, these findings identify HDAC1 as a potential epigenetic regulator of chemosensitivity in breast cancer and a candidate prognostic biomarker and therapeutic target.

Materials and Methods

1. Expression analysis of HDAC1 in breast cancer

We systematically analyzed the expression patterns of HDAC1 in breast cancer using multiple public databases. All analyses of HDAC1 mRNA and protein expression were obtained through the UALCAN online analysis portal (http://ualcan.path.uab.edu/analysis.html)[22], which provides comprehensive cancer transcriptome analysis. UALCAN provides standardized access to TCGA[23] and CPTAC databases. The UALCAN portal normalizes logged expression values to standard deviations from the median in each proteomic profile. HDAC1 expression changes across breast cancer were visualized using R software (Version 4.0.2; https://www.Rproject.org). The HPA, (https://www.proteinatlas.org/) was used to download the immunohistochemical staining of HDAC1 protein expression. Representative tissue microarrays showing HDAC1 protein expression in adjacent normal tissue, ductal carcinoma, and lobular carcinoma were retrieved and analyzed.

For survival analysis, we extracted overall survival (OS) data from TCGA datasets. Based on HDAC1 expression levels, patients were stratified into high and low expression groups using the median expression value as the cutoff. Subsequently, the association between HDAC1 and survival was evaluated using Kaplan-Meier curves and log-rank tests.

2. Identification of drug sensitivity-associated genes and functional enrichment analysis

To identify genes associated with drug sensitivity in breast cancer, we systematically curated three independent gene expression datasets from the GEO database that contained samples with documented differential drug-response phenotypes. The datasets included GSE76540, GSE104050, and GSE41998, all of which contained breast cancer samples with paired drug-sensitive and drug-resistant groups. We performed Venn diagram analysis using the "VennDiagram" R package to identify overlapping genes among these datasets. A total of 391 common DEGs were identified as drug sensitivity-associated DEGs.

Cancer hallmark enrichment analysis for HDAC1 was conducted using the Molecular Signatures Database (MSigDB) to evaluate the association between HDAC1 expression and core cancer biological processes. Totally, we assessed enrichment across nine hallmark gene sets.

Functional enrichment analysis was performed using the 391 common DEGs identified from the three GEO datasets. Kyoto Encyclopedia of Genes and Genomes (KEGG) pathway enrichment analysis was conducted to identify biological pathways associated with these drug sensitivity-associated DEGs, while Gene Ontology (GO) enrichment analysis was performed to characterize their functional features across the biological process (BP), molecular function (MF), and cellular component (CC) categories. GO and KEGG enrichment analyses were performed using the “clusterProfiler” R package, with adjusted $P<0.05$ considered statistically significant after Benjamini–Hochberg correction for multiple testing. The enrichment results were visualized using the “GOplot” R package.

3. Construction and validation of HDAC1 overexpressing recombinant lentiviral vectors

To construct the HDAC1 overexpression lentiviral vector, total RNA was extracted from

MCF-7 cell lines and subjected to RT-PCR amplification. The PCR-amplified HDAC1 fragment was cloned into the pSIMPLE-18 T vector to generate the recombinant plasmid pSIMPLE-18T-HDAC1. The ligation products were transformed into Escherichia coli (E. coli) DH5α competent cells, and positive clones were screened and verified by XbaI/EcoRI double digestion. The confirmed HDAC1 fragment was subsequently inserted into the pCDH-CMV-MCS-HDAC1-EF1-Puro lentiviral vector. The corresponding empty vector was used as a negative control. Recombinant plasmids were further confirmed by XbaI/EcoRI double digestion and sequencing.

Recombinant lentivirus was generated by transient transfection of 293T cells with the recombinant lentiviral vector expression vector together with the packaging plasmids pMDLg/pRRE, pRSV-Rev, and pMD 2.G. Viral supernatants were collected at 24 h, 28 h, 32 h, 36 h, 48 h post-transfection, clarified to remove cellular debris, and used to infect MCF-7 cells. In parallel, an empty vector containing a noncoding sequence was used to produce control lentivirus. After 4 weeks of selection with 2 μg/mL puromycin, a stable HDAC1-overexpressing MCF-7 cell line was finally established.

The MCF-7 cell line was obtained from the Tumor Cell Bank at the Chinese Academy of Medical Sciences. MCF-7 serial number: TCHu 74; URL: https://cellbank.org.cn/search-detail.php?id=152. The identity of the cell lines was verified based on their characteristic morphology and growth properties before experimentation. In addition, all cell lines were routinely tested and confirmed to be free of mycoplasma contamination prior to experimentation. MCF-7 is a luminal A–like, hormone receptor–positive breast cancer cell line that closely reflects the clinical and molecular features of this subtype and is widely used to study tumor cell survival, apoptosis, and responses to chemotherapy. MCF-7 cells were selected due to their well-characterized chemosensitivity and suitability for modeling epigenetic regulation in breast cancer.

4. Western blot analysis of the effect of recombinant lentiviral vector transfection on HDAC1 protein expression in MCF-7 cells.

The stably transfected MCF-7-HDAC1 and MCF-7-control cells were lysed for total protein extraction and concentration determination. Equal amounts (30μg per lane) were loaded onto a 15% SDS-PAGE gel. Proteins were transferred at 4°C for 2h, the membrane blocked at room temperature for 2h, and incubated with anti–HDAC1 primary antibody overnight at 4℃. After washing, the membrane was incubated with the

appropriate secondary antibody for 2h at room temperature, washed again, treated with ECL substrate, developed for 2min, and imaged by chemiluminescence imaging system for Western blot analysis (Clinx, Shanghai, China).

5. Effect of HDAC1 overexpression on chemosensitivity to chemotherapeutic agents in breast cancer cells.

5.1 Experimental groups and treatment protocol.

To investigate the relationship between HDAC1 overexpression and chemosensitivity in breast cancer, MCF-7 cells stably overexpressing HDAC1 (MCF-7-HDAC1) and corresponding control cells (MCF-7-Control) were assessed. Each cell line was allocated to four treatment groups: untreated control (Control) group, VM-26 group, DDP group and THP group. Specifically, control cells were maintained in DMEM supplemented with 10% FBS. For treatment groups, cells in the THP group were treated at three final concentrations of 0.39, 0.78, and 1.56 μg/mL for 72 h. VM-26 group at 0.39, 0.78, 1.56, and 3.12 μg/mL for 48 h; and DDP group at 0.3125, 0.625, 1.25, and 2.5 μg/mL for 48 h. THP was dissolved in sterile water, VM-26 in dimethyl sulfoxide (DMSO), and DDP in phosphate-buffered saline (PBS).

These three drugs were selected as representative chemotherapeutic agents with distinct mechanisms of action, allowing us to assess whether HDAC1 overexpression reduces chemosensitivity to multiple chemotherapeutic agents in MCF-7 cells. THP acts through DNA intercalation and topoisomerase II inhibition, whereas VM-26 and DDP induce DNA damage by stabilizing topoisomerase II-DNA cleavage complexes and forming DNA crosslinks, respectively. The drug concentrations and incubation times were determined based on preliminary dose–response experiments and corresponding IC_{50} values, and were consistent with conditions reported in previous studies [24,25].

5.2 Assessment of the effect of HDAC1 overexpression on MCF-7 cell viability by the MTT assay.

Cells in the logarithmic growth phase were seeded into 96-well plates at a density of 3×10^3 cells per well, with four technical replicates for each of the MCF-7-HDAC1 and MCF-7-Control groups. After 48-72 h of incubation, MTT solution (0.5%, 20 μL per well) was added for 4 h, followed by dissolution of formazan crystals in DMSO and measurement of absorbance at 490 nm to assess cell viability.

5.3 Assessment of Apoptosis in HDAC1-Overexpressing MCF-7 Cells by Hoechst

33258/PI Double Staining

MCF-7-HDAC1 and MCF-7-Control cells in the logarithmic growth phase were seeded in 24-well plates at 5×10^4 cells per well. After 48-72 h of drug treatment, cells were washed twice with phosphate-buffered saline and sequentially stained with Hoechst 33258 (100 μL, 37°C, 15 min, dark) and PI (100 μL, 4°C, 10 min, dark), followed by imaging using fluorescence microscopy (Nikon, Tokyo, Japan) (Hoechst: blue; PI: red).

5.4 Flow cytometric analysis of the effect of HDAC1 overexpression on apoptosis in MCF-7 cells.

MCF-7-HDAC1 and MCF-7-Control cells in the logarithmic growth phase were seeded into 6-well plates at 2×10^5 cells per well. Following 48-72h of drug treatment, cells were resuspended in 1× binding buffer, adjusted to 1×10^5 cells per 100 μL, stained with Annexin V-FITC and PI for 15 min at room temperature in the dark, and immediately analyzed by BD FACSCalibur™ flow cytometer (BD Biosciences, San Jose, CA, USA) (FITC = green; PI = red).

6. Construction of the HDAC1 protein–protein Interaction network and pathway-specific expression analysis in breast cancer

To investigate the molecular interactions and pathway-specific expression patterns of HDAC1 in breast cancer, we performed comprehensive bioinformatic analyses using multiple public datasets. For the PPI network construction, we utilized the STRING database[26] (version 11.0; https://string-db.org/) with a confidence score threshold of 0.7. The network was visualized and analyzed using cytoscape software (version 3.8.2), with node size proportional to degree centrality and edge width representing interaction confidence. Functional enrichment analysis of the HDAC1-associated network was performed using the Database for Annotation, Visualization and Integrated Discovery (DAVID) to identify enriched biological processes and pathways.

The potential interaction between HDAC1 and YY1 was investigated by protein–protein docking using HADDOCK, with human HDAC1 (PDB ID: 4BKX; structural Zn^{2+} retained) and full-length human YY1 (UniProt P25490; AlphaFold model) used as Protein A and Protein B, respectively. The selected docking complex was evaluated using PDBePISA and visualized in PyMOL 3.0.3 to characterize the predicted binding interface and interacting residues. A 100-ns molecular dynamics simulation was performed to assess complex stability and conformational dynamics based on RMSD,

RMSF, Rg, SASA, and intermolecular hydrogen bonding, together with a three-dimensional free-energy landscape based on RMSD and Rg. MM-PBSA analysis was further used to estimate the binding free energy of the HDAC1–YY1 complex.

7. Pathway-specific analysis of HDAC1 protein expression in breast cancer

To examine HDAC1 expression in relation to specific molecular pathways, we leveraged the CPTAC dataset through the UALCAN web portal. The CPTAC dataset contains proteomic profiles of breast cancer samples with comprehensive molecular annotation. We specifically analyzed HDAC1 protein expression across different molecular subgroups: including Chromatin modifier status, p53/RB1 pathway status and NRF2 pathway status. We systematically assessed pathway-level somatic alterations (by small mutation or copy number alteration) across tumors with combined proteomic, whole-exome, and CNA data, involving key pathways and genes previously annotated across multiple cancer types based on domain knowledge (pathway annotations from PMID: 33568653). Log2 Spectral count ratio values from CPTAC were first normalized within each sample profile, then normalized across samples.

8. Analysis of HDAC1 expression in relation to immune cell infiltration

To evaluate the association between HDAC1 expression and the tumor microenvironment (TME), the "ESTIMATE" R package was employed to calculate the immune, stromal, and ESTIMATE scores for each breast cancer patient based on HDAC1 gene expression. The estimation of stromal and immune cells in malignant tumor tissues using expression data (ESTIMATE) algorithm employs gene expression signatures to infer the relative proportions of stromal and immune cells in tumor samples. Additionally, Spearman's correlation coefficient between HDAC1 expression and immune infiltration scores across breast cancer was computed using the corr.test function from the R package psych.

To further characterize immune cell composition, the TIMER algorithm implemented in the R package IOBR was used to estimate the infiltration levels of six immune cell types in breast cancer samples based on gene expression data, including B cells, $CD4^+$ T cells, $CD8^+$ T cells, neutrophils, macrophages, and dendritic cells. Pearson's correlation coefficients between gene expression and immune cell infiltration levels were calculated using the corr.test function in the R package psych (version 2.1.6) to identify significantly associated immune cell populations [27].

9. Analysis of immune checkpoint gene expression and correlation with HDAC1.

The most frequently utilized drugs in immunotherapy target and inhibit immune checkpoint pathways, thereby aiding the immune system in overcoming immune evasion mediated by checkpoint overexpression and reactivating immune responses against neoantigen-expressing cancer cells. Therefore, we performed an immune checkpoint analysis to investigate the associations between HDAC1 expression and immune checkpoint-associated genes. Furthermore, expression data for 24 inhibitory immune checkpoint pathway genes were extracted for each sample. The relationship between HDAC1 expression and immune checkpoint genes was analyzed using Spearman's correlation, with the results visualized through a heatmap.

10. Statistical analysis

R software was used in the bioinformatics analysis in this study. Student's t-test was used to compare the expression levels of HDAC1 between different groups, and the Wilcoxon rank-sum test was used to analyze non-normally distributed data. An unpaired two-sample t-test was used to assess differences in expression between two groups, while one-way ANOVA was applied for comparisons among multiple groups. For the wet lab experiment performed in this study, homogeneity of variance was assessed prior to ANOVA. Pearson correlation analysis was employed to evaluate the correlation between HDAC1 expression and immune infiltration. SPSS 26.0 software was used. P-values < 0.05 were considered significant.

The principal reagents and materials used in this study are listed in **Table 1**.

Results

1. HDAC1 expression is significantly upregulated in breast cancer.

Analysis of HDAC1 expression based on TCGA dataset revealed significantly elevated mRNA levels in primary breast cancer tissues compared with normal breast tissues ($P < 0.01$ vs. Normal; **Figure 1A**). Analysis of HDAC1 expression across clinical stages demonstrated a progressive upregulation from stage I to stage IV, with stage IV tumors exhibiting the highest expression levels (all $P < 0.05$ vs. Normal; **Figure 1B**). Further analysis across the major molecular subtypes of BRCA, including triple-negative breast cancer (TNBC) subtypes, demonstrated pronounced heterogeneity in expression patterns. Compared with normal tissues, HDAC1 expression was significantly elevated in Luminal, TNBC-BL1, TNBC-BL2, TNBC-IM, TNBC-M, TNBC-MSL and TNBC-UNS

subtypes (all $P < 0.05$ vs. Normal), while notably reduced in HER2-positive and TNBC-LAR subtypes (**Figure 1C**). Immunohistochemical (IHC) staining results from the Human Protein Atlas (HPA) database demonstrated higher HDAC1 expression in breast tissues than in adjacent normal tissues (**Figure 1D**). Notably, IHC staining revealed more intense HDAC1 expression in lobular carcinoma than in ductal carcinoma. (**Figure 1D**). Consistent with the transcriptomic findings, proteomic data confirmed that HDAC1 protein levels were significantly elevated in primary BRCA tissues compared with normal tissues ($P < 0.01$; **Figure 1E**). Kaplan–Meier survival analysis based on TCGA datasets demonstrated that high HDAC1 expression was significantly associated with poorer overall survival (OS) in patients with BRCA (HR = 1.43, 95% CI: 1.03-1.99; **Figure 1F**).

Collectively, these findings indicate that HDAC1 is upregulated in BRCA, and that HDAC1 overexpression is associated with poor clinical outcomes, highlighting HDAC1 potential as a prognostic biomarker and therapeutic target.

2. Identification and functional enrichment analysis of drug sensitivity-associated DEGs in breast cancer.

To systematically characterize the role of HDAC1 in breast cancer drug sensitivity, we integrated three GEO datasets comprising breast cancer samples with documented drug-sensitive and drug-resistant phenotypes (**Table 2**). Venn diagram analysis identified 391 common DEGs (**Figure 2A**). Further cancer hallmark enrichment analysis revealed that HDAC1 is centrally associated with malignant phenotypes, including enhanced proliferation, invasion, genomic instability, and, most notably, resistance to cell death (**Figure 2B**).

Subsequently, KEGG pathway enrichment analysis was conducted to investigate the signaling pathways associated with HDAC1 in breast cancer. KEGG analysis revealed significant enrichment of several cancer-associated pathways, notably the p53 signaling pathway, suggesting that HDAC1 may contribute to reduced drug sensitivity through modulation of apoptosis and cell-cycle related signaling networks (**Figure 2C**). GO BP functional enrichment analysis further indicated that HDAC1 is involved in positive regulation of apoptosis process, negative regulation of cell population proliferation, and negative regulation of cell migration (**Figure 2D**).

Collectively, integrative analysis of three GEO datasets identified HDAC1 as a drug

sensitivity-associated gene in breast cancer, with elevated expression in less sensitive samples and enrichment in malignant phenotypes and biological processes related to apoptosis, cell proliferation, and migration.

3. Construction and characterization of the HDAC1 overexpression recombinant lentiviral vector.

To investigate the role of HDAC1 in breast cancer chemosensitivity, the full-length HDAC1 coding sequence was amplified by PCR and subcloned into a lentiviral expression vector (**Figure S1**); primer sequences are provided in **Table 3**. PCR amplification produced a single band of approximately 1,449 bp, consistent with the expected size of the target fragment (**Figure 3A**). Restriction enzyme digestion of the recombinant plasmid pSIMPLE-18T-HDAC1 generated two fragments of approximately 2,700 bp and 1,449 bp, confirming successful cloning (**Figure 3B**). Double digestion of XbaI/EcoRI and sequencing of the recombinant lentiviral construct pCDH-CMV-MCS-HDAC1-EF1-Puro revealed two bands of 7400 bp and 1449 bp, consistent with the expected insert size (**Figure 3C**). Western blot demonstrated the overexpression of HDAC1 protein in the MCF-7-HDAC1 group compared with the MCF-7-Control group (**Figure 3D**).

Collectively, a stable HDAC1-overexpressing MCF-7 cell line was established and validated at both the genetic and protein levels, providing an experimental model suitable for subsequent functional studies of HDAC1 in breast cancer chemosensitivity.

4. Overexpression of HDAC1 reduces chemosensitivity and inhibits apoptosis in MCF-7 breast cancer cells.

To assess the impact of HDAC1 overexpression on chemosensitivity, MCF-7-HDAC1 and MCF-7-Control cells were treated with increasing concentrations of THP, VM-26, and DDP for 48 or 72 h. MTT assays showed a dose-dependent reduction in cell viability in both cell lines, with HDAC1-overexpressing cells consistently exhibiting moderately higher viability than control cells following drug treatment (**Figures 3F–H**). Accordingly, IC_{50} values for THP, VM-26, and DDP were increased in MCF-7-HDAC1 cells compared with controls (0.822 vs. 0.514 μg/mL for THP; 1.886 vs. 1.490 μg/mL for VM-26; and 1.831 vs. 1.158 μg/mL for DDP), indicating a modest but reproducible reduction in chemosensitivity.

Hoechst 33258/propidium iodide (PI) staining further revealed increased nuclear

abnormalities and PI-positive nuclei following drug exposure in MCF-7-Control cells, whereas MCF-7-HDAC1 cells exhibited fewer nuclear abnormalities and reduced PI positivity, consistent with a modest attenuation of chemotherapy-induced cell death. (**Figures 4A–C**).

Flow cytometric analysis demonstrated dose-dependent apoptosis in both groups; however, the apoptotic fraction was significantly lower in MCF-7-HDAC1 cells across all tested concentrations ($P < 0.05$; **Figures 5A–F**). For instance, THP treatment resulted in reduced apoptosis in HDAC1-overexpressing cells compared with controls (3.01% vs. 5.42%, 13.23% vs. 24.63%, 18.79% vs. 38.78%, and 39.4% vs. 52.67% across increasing doses; $P < 0.01$), with similar trends observed for VM-26 (7.66% vs. 5.86%, 18.13% vs. 25.96%, 26.77% vs. 33.8%, and 39.6% vs. 50.2% across increasing doses; $P < 0.01$) and DDP (7.98% vs. 6.29%, 13.21% vs.18.66%, 17.78% vs. 24.86%, and 30.19% vs. 53.6% across increasing doses; $P < 0.001$) .

Overall, HDAC1 overexpression in MCF-7 cells was associated with increased IC_{50} values and reduced apoptosis, supporting a modest but consistent role for HDAC1 reducing chemosensitivity through enhanced cell survival and suppression of apoptotic responses.

5. HDAC1 is associated with chemotherapy response and shows a predicted interaction with YY1.

To further investigate the potential mechanistic framework underlying HDAC1-associated chemosensitivity in breast cancer, a protein–protein interaction (PPI) network centered on HDAC1 was constructed. The resulting network identified several prominent interacting partners, including methyl-CpG binding domain protein 2 (MBD2), snail family transcriptional repressor 1 (SNAI1), C-terminal binding protein 1 (CTBP1), E1A binding protein p300 (EP300), and Yin Yang 1 (YY1), all of which have been implicated in tumor plasticity and chemosensitivity. Notably, the canonical tumor suppressors tumor protein p53 (TP53) and retinoblastoma protein 1 (RB1) also emerged as central nodes within the PPI network (**Figure 6A**).

To further examine the potential interaction between HDAC1 and YY1, protein–protein docking was performed. The predicted complex yielded a docking score of -9.6 kcal/mol and showed an extensive interaction interface, with 11 hydrogen bonds and two salt bridges involving residues from both proteins (Figure **6B–C**).

Further molecular dynamics simulation further supported the stability of the docked complex. Following an initial conformational adjustment, RMSD remained within approximately 1.3-1.5 nm, with relatively low residue-level fluctuations across most of the complex (**Figure 7A, B**). During the 100-ns simulation, *R*g decreased from approximately 4.3 to 3.6 nm, while intermolecular hydrogen bonding was maintained at relatively high levels and SASA decreased from approximately 590 to 400 nm² (**Figure 7C–E**). The free-energy landscape showed that the complex converged toward a limited set of low-energy conformations (**Figure 7F**), supporting a compact and relatively stable HDAC1–YY1 complex throughout the latter phase of the simulation. Collectively, Collectively, HDAC1 was identified as a central node in a protein-protein interaction network comprising key regulators of tumor therapeutic response and the computational analyses provide structural evidence supporting a potential interaction between HDAC1 and YY1 and provide a structural basis for subsequent experimental validation.

6. HDAC1 is upregulated in breast tumors with aberrant chromatin modification and dysregulated p53/RB1 and NRF2 signaling.

Analysis of the CPTAC dataset revealed that HDAC1 is significantly overexpressed in breast tumors exhibiting aberrant chromatin modification patterns in breast cancer (all P <0.05 vs. Normal or Others; **Figure 8A**). Furthermore, HDAC1 expression is markedly upregulated in breast tumors exhibiting dysregulation of the p53/RB1 pathways (all P <0.05 vs. Normal or Others; **Figure 8B**). Moreover, HDAC1 was markedly upregulated in breast tumors exhibiting activation of the nuclear factor erythroid 2–related factor 2 (NRF2) pathway (all P <0.05 vs. Normal or Others; **Figure 8C**). Collectively, HDAC1 was markedly overexpressed in breast tumors exhibiting aberrant chromatin modifications, P53/RB1 pathway dysregulation, and NRF2 pathway activation.

7. HDAC1 modulates tumor microenvironment and immune checkpoint interactions in breast cancer.

Immune infiltration analysis demonstrated that HDAC1 expression was significantly negative correlated with the stromal score (R=-0.21, P=1.5e-12), immune score (R=-0.12, P=8.1e-5), and ESTIMATE score (R=-0.18, P=1.7e-9) in BRCA (**Figure 9A-C**). The correlation analysis between HDAC1 and 24 inhibitory immune checkpoint genes across breast cancer samples revealed complex patterns of interaction (**Figure 9D**), with HDAC1 showing strong positive correlations with several inhibitory checkpoint molecules including cytotoxic t-lymphocyte associated protein 4 (CTLA4), hepatitis a

virus cellular receptor 2 (HAVCR2), and programmed cell death 1 (PDCD1). Consistent with a selective effect on immune composition, HDAC1 expression showed statistically significant positive correlations with several immune cell types estimated in BRCA (**Figure 9E**), including B cells (R=0.07, P=0.02), $CD4^+$ T cells (R=0.12, P=6.0e-5), $CD8^+$ T cells (R=0.09, P=3.9e-3), neutrophils (R=0.13, P=2.1e-5), and dendritic cells (DC) (R=0.11, P=3.1e-4). These findings highlight the intricate relationship between HDAC1 and immune regulation in breast cancer, suggesting that HDAC1 may play a role in shaping the tumor immune landscape and potentially contributing to immunosuppressive mechanisms that could influence chemotherapy response.

Discussion

In this study, we provide evidence that HDAC1 reduces chemosensitivity in luminal A breast cancer. HDAC1 was significantly upregulated in breast cancer tissues and associated with chemosensitivity-related gene signatures. Functional and pathway analyses, together with in vitro assays, indicated that HDAC1 promotes cell survival and suppresses chemotherapy-induced apoptosis, potentially through chromatin remodeling and dysregulated p53/RB1- and NRF2-associated signaling, with the potential involvement of YY1. Moreover, HDAC1 expression was associated with tumor microenvironment alterations, including immune cell infiltration and immune checkpoint-related gene expression, suggesting that HDAC1 may influence chemosensitivity through both tumor cell-intrinsic and tumor-immune mechanisms.

Histone deacetylases (HDACs) are frequently located in chromosomal regions prone to genetic alterations and have been implicated in the initiation and progression of breast cancer[28]. Among class I HDACs, HDAC1 is closely associated with tumorigenesis and regulates multiple biological processes in breast cancer [7,8,10,29]. HDAC1 is frequently upregulated in advanced, poorly differentiated, and highly proliferative tumors, including breast cancer [11]. In breast cancer, increased HDAC1 mRNA expression has been consistently observed in tumor tissues compared with adjacent normal tissues [30,31] and, in a subset of cases, is associated with adverse clinical outcomes[32]. In the present study, we likewise found that HDAC1 was significantly overexpressed in breast cancer and was associated with poor prognosis. Notably, our functional studies in MCF-7 cells, a Luminal A breast cancer model, further showed that HDAC1 overexpression reduced the response to multiple chemotherapeutic agents by promoting cell survival and suppressing drug-induced apoptosis. These findings extend the potential role of HDAC1 beyond

tumor progression to the regulation of chemotherapy response in Luminal A breast cancer. Accordingly, a range of HDAC inhibitors have been developed and evaluated as anticancer agents in solid and hematologic malignancies [19,33,34]. By inhibiting HDAC activity, these agents may restore the expression of silenced tumor suppressor genes and promote cancer cell death, raising the possibility that HDAC1 inhibition could also improve chemotherapy sensitivity.

To further delineate the functional role of HDAC1 in breast cancer, we conducted cancer hallmark pathway enrichment analyses, which demonstrated that HDAC1 is strongly associated with multiple malignant phenotypes, including increased cell proliferation, invasive capacity, genomic instability, and, most notably, resistance to programmed cell death. Consistently, GO enrichment analysis indicated that HDAC1 is involved in the regulation of apoptosis, negative regulation of cell proliferation, and promotion of cell migration. Accumulating evidence indicates that HDAC1 targeting mediated repression, genetic silencing, or pharmacological inhibition—reduces breast cancer cell aggressiveness by suppressing migration and proliferation while promoting apoptosis and immunogenic cell death[9,10,35]. Conversely, HDAC1 overexpression substantially enhances the invasive capacity of MCF-7 breast cancer cells[7]. Our study further demonstrated that HDAC1 overexpression promotes cell proliferation and suppresses chemotherapy-induced apoptosis. Collectively, HDAC1 overexpression is associated with enhanced Luminal A breast cancer cell proliferation and invasion, reduced chemosensitivity, and suppressed apoptosis.

Further KEGG enrichment analysis and PPI network analysis revealed that HDAC1 interacts with the key tumor suppressors TP53 and RB1. As central intracellular "guardians" of genomic integrity, the p53/RB1 pathway plays a pivotal role in regulating apoptosis in breast cancer[16,17]. Functional inactivation of this pathway leads to widespread disruption of cell-cycle checkpoints, senescence, and apoptosis in response to DNA damage, thereby allowing damaged cells to evade effective elimination. Collectively, these findings suggest that HDAC1 may contribute to at least in part, through modulation of critical tumor-suppressive pathways governing cell-cycle progression and apoptotic responses[36]. Furthermore, proteomic analyses of patient samples demonstrated that HDAC1 is significantly upregulated in breast tumors exhibiting p53/RB1 pathway dysregulation compared with adjacent normal tissues, suggesting that HDAC1 may regulate apoptotic processes in breast cancer through

519 modulation of the p53/RB1.

520 Accumulating evidence indicates that pharmacological or genetic inhibition of HDAC1
521 suppresses breast cancer progression by modulating apoptosis and cell proliferation;
522 moreover, inhibition of histone deacetylases, including HDAC1, has been shown to
523 restore and enhance sensitivity to anti-estrogen therapy in breast cancer[37,38]. However,
524 the precise molecular mechanisms underlying HDAC1-mediated regulation of
525 chemosensitivity in breast cancer remain largely undefined. Therefore, by constructing
526 an HDAC1-centered PPI network, we identified several key regulators associated with
527 chemosensitivity that interact with HDAC1, including MBD2, SNAI1, CTBP1, EP300,
528 and YY1. MBD2 facilitates tumor progression by recruiting the NuRD chromatin-
529 remodeling complex to specific genomic loci to enforce transcriptional repression[39], and
530 as HDAC1 serves as a core catalytic subunit of NuRD conferring a critical synthetic-
531 lethal dependency in cancer[40], inhibition of MBD2 has been shown to suppress ABCB1
532 expression and significantly reduce cisplatin resistance in cholangiocarcinoma cells [41].
533 As a transcriptional repressor, SNAI1 directly recruits epigenetic modifiers such as
534 HDAC1 to assemble transcriptional repressive complexes [42], thereby driving epithelial–
535 mesenchymal transition (EMT)[43] and promoting tumor invasion, metastasis, stemness,
536 and responses to chemotherapy. Emerging evidence further indicates that SNAI1
537 enhancer RNA (SNAI1e) activates TGF-β/SMAD signaling to reinforce these
538 phenotypes in breast cancer cells[44]. CTBP1 as a transcriptional corepressor by recruiting
539 epigenetic modifiers such as HDAC1 to gene promoters to form repressive chromatin
540 complexes that silence tumor suppressor genes and drive tumor initiation and
541 progression[45]. CTBP1 has also been shown to promote chemoresistance in breast cancer
542 through both p53-dependent and -independent mechanisms[46].This effect is mediated in
543 part by transactivation of RAD51[47], whereas genetic ablation or miR-644a–mediated
544 repression of CTBP1 markedly suppresses tumor growth, metastasis, and therapeutic
545 resistance[48]. P300 and HDAC1 oppositely regulate histone acetylation to control
546 chromatin structure and gene transcription, and disruption of this balance during
547 tumorigenesis cooperatively drives malignant phenotypes[49], while EP300 has been
548 identified as a tumor suppressor that modulates paclitaxel resistance and cancer stemness
549 in breast cancer[50]. functional integration of TP53 and RB1 with the central epigenetic
550 regulator HDAC1 through transcriptional repressor complexes and consequent
551 hyperactivation of the RB1–HDAC1 axis upon TP53 loss drive genomic instability,
552 malignant progression, and resistance to DNA damage–inducing therapies, including

553 doxorubicin and platinum-based chemotherapies [51,52]. Moreover, YY1 can recruit
554 HDAC1 into transcriptional repressor complexes, thereby contributing to the silencing
555 of tumor suppressor and differentiation programs and the activation of pathways
556 associated with drug efflux, stemness, DNA repair, microenvironmental remodeling, and
557 EMT, all of which have been implicated in tumor progression and therapeutic resistance[53].
558 To further explore the potential interaction between HDAC1 and YY1, we performed
559 computational structural analyses, which predicted a favorable and relatively stable
560 HDAC1–YY1 complex and identified several candidate residues at the protein–protein
561 interface. Taken together, these findings suggest that HDAC1 may contribute to
562 chemoresistance in breast cancer through its association with multiple regulatory
563 proteins, including MBD2, SNAI1, CTBP1, EP300, and YY1, while the structural
564 analyses provide additional support for a potential HDAC1–YY1 interaction.

565 CPTAC proteomic profiling revealed marked upregulation of HDAC1 in breast tumors
566 with aberrant chromatin states and activated NRF2 signaling. Chromatin modifications
567 drive tumor drug resistance, as cancer cells dynamically remodel chemical marks and
568 chromatin structure to reprogram gene expression, evade cytotoxic drugs, and acquire
569 resistance[54]. Chromatin modification patterns given that changes in histone
570 acetylation/methylation can activate oncogenes and silence tumor suppressors, this
571 upregulation supports a model in which HDAC1 enhances epigenetic plasticity to
572 promote drug resistance. The NRF2 (Nrf2/KEAP1) pathway promotes chemoresistance
573 in breast cancer through activation of antioxidant and drug-metabolizing programs, and
574 concomitant HDAC1 upregulation in NRF2-activated tumors further exacerbates
575 treatment resistance[55-57]. In summary, HDAC1 integrates chromatin remodeling, tumor
576 suppressor dysfunction, and stress-response signaling to drive breast cancer progression
577 and chemoresistance, highlighting HDAC1 inhibition as a potential strategy to improve
578 responses to conventional therapies.[58].

579 The tumor immune microenvironment (TIME) is a central determinant of therapeutic
580 response in breast cancer, and dysregulation of the TIME may contribute to reduced
581 chemosensitivity by promoting immune evasion and attenuating chemotherapy-induced
582 immune responses. Neutrophils have emerged as key mediators of resistance [59], with
583 $CD4^+$ T cell–driven neutrophil ferroptosis fostering immunosuppression[60], s senescent
584 neutrophil–derived exosomal piRNA-17560 promotes epithelial–mesenchymal
585 transition and chemoresistance via the FTO–ZEB1 axis[61], and benzyl butyl phthalate

(BBP) potentiates the pro-chemoresistant effects of tumor-associated dendritic cells in breast cancer [62]. Consistent with these observations, ESTIMATE and TIMER analyses demonstrated that HDAC1 expression is inversely associated with overall immune and stromal infiltration, while showing positive correlations with $CD4^+$ T cells, neutrophils, and dendritic cells in breast cancer, indicative of context-dependent immune microenvironment remodeling. Mechanistically, HDAC1-mediated chromatin regulation critically shapes both innate and adaptive immune programs, including control of $CD4^+$ T-cell plasticity[63] and neutrophil differentiation whereas HDAC inhibition suppresses neutrophil progenitor expansion, induces apoptosis, promotes dendritic cell maturation [64] , and enhances immunogenic cell death and T-cell activation, collectively eliciting robust antitumor immune responses [65]. These findings suggest that HDAC1 may contribute to reduced chemosensitivity in breast cancer through alterations in immune cell composition and function, thereby suppressing antitumor immunity and potentially attenuating chemotherapy-induced immune responses. Emerging evidence indicates that combining chemotherapy with immune checkpoint blockade may enhance treatment sensitivity and limit tumor progression and metastasis[66], as multiple immune checkpoints, including PD-1/PD-L1, CTLA-4, B7-H3, B7-H4, B7-1, and B7-2, act as positive regulators of multidrug resistance in breast cancer[67]. Consistently, Spearman correlation analysis revealed strong positive associations between HDAC1 expression and inhibitory immune checkpoints, including PDCD1 and CTLA4. Tumor immune evasion is mediated in part through programmed cell death protein 1 (PD-1, encoded by PDCD1)/ programmed death-ligand 1 (PD-L1) and CTLA-4 signaling, which suppress T-cell activation and function[68,69], and these pathways have emerged as effective targets for immune checkpoint blockade[70] and promising immunotherapeutic strategies in breast cancer [71-73]. Collectively, these findings indicate that HDAC1 may be associated with reduced chemosensitivity in breast cancer through modulation of the tumor immune microenvironment, including neutrophil- and dendritic cell-mediated immunosuppression and upregulation of inhibitory immune checkpoint pathways, such as PD-1/PD-L1 and CTLA-4, thereby potentially facilitating immune evasion and attenuating antitumor immunity while supporting the rationale for combined HDAC-targeted and immunotherapeutic strategies.

Despite the insights provided by the present study, several limitations should be acknowledged. MCF-7 cells were used as a representative model of hormone receptor–positive breast cancer, owing to their stable growth properties and preserved apoptotic

responses, which allow consistent evaluation of HDAC1-associated effects on cell survival and apoptosis. In addition, their relatively high baseline chemosensitivity facilitates the detection of treatment-induced reductions in chemosensitivity. However, this model does not fully reflect the biological heterogeneity of breast cancer, particularly more aggressive subtypes such as triple-negative disease. Given potential subtype-specific differences in HDAC1-related signaling, validation in additional cell models will be necessary to assess the broader applicability of these findings. In addition, the functional analyses were primarily based on an HDAC1 overexpression system, without complementary loss-of-function validation, which would strengthen causal inference. Although bioinformatic analyses linked HDAC1 to multiple pathways associated with reduced chemosensitivity and computational modeling supported a potential HDAC1–YY1 interaction, these findings remain largely predictive, and their underlying molecular mechanisms require further experimental validation. Finally, experimental validation was restricted to in vitro models, and in vivo studies are required to confirm these findings. Future investigations incorporating genetic perturbation strategies and animal models will be essential to further define the role of HDAC1 in breast cancer chemosensitivity and assess its therapeutic potential.

Conclusions

Overall, our findings indicate that HDAC1 overexpression is associated with reduced chemosensitivity in Luminal A breast cancer cells. In MCF-7 cells, HDAC1 overexpression decreased the response to THP, VM-26, and DDP by promoting cell survival and suppressing drug-induced apoptosis. HDAC1 may contribute to chemoresistance through coordinated regulation of chromatin remodeling and chemotherapy response-associated signaling pathways, including the p53/RB1 and NRF2 axes. Computational structural analyses supported a potential interaction between HDAC1 and YY1, suggesting that the HDAC1–YY1 axis may be involved in the regulation of chemosensitivity. Collectively, these findings support HDAC1 as a potential prognostic biomarker and therapeutic target and provide a basis for further investigation of HDAC1-directed strategies in combination with chemotherapy.

Abbreviations

Abbreviation	Full name
bp	Base pair
BRCA	Breast invasive carcinoma

BSA	Bovine serum albumin
cDNA	Complementary deoxyribonucleic acid
CMV	Cytomegalovims
DDP	cis-dichlorodiamineplatinum
DEGs	Differentially expressed genes
DMEM	Dulbecco's modified eagle's medium
ECL	Enhanced chemiluminescence
EF-1	Elongation factor-1
ESTIMATE	Estimation of stromal and immune cells in malignant tumour tissues using expression data
FBS	Fetal bovine serum
FITC	Fluorescein isothiocyante
GFP	Green fluorescent protein
HAT	Histone acetyl transferase
HER-2	Human epidermal growth factor receptor 2
HDAC	Histone deacetylase
HDACi	Histone deacetylase inhibitor
HPA	Human protein atlas
IHC	Immunohistochemical
MTT	3-(4,5-dimethylthiazol-2-yl)-2,5-diphenyltetrazolium bromide
NRF-2	Nuclear factor erythroid 2-related factor 2
PCR	Polymerase chain reaction
PI	Propidium iodide
RB1	Retinoblastoma 1
RT-PCR	Reverse Transcription-polymerase chain reaction
SDS-PAGE	Sodium dodecyl sulfate polyacrylamide gel electrophoresis
THP	Pirarubicin
TNBC	Triple-negative breast cancer
VM-26	Teniposide

Acknowledgements

Not applicable.

Funding Statement

This work was supported by The National Natural Science Foundation for Young Scientists of China (Grant No. 30701030); The Tianjin Application Foundation and Advanced Technology Research Program of China (Grant No. 11JCYBJC14900); The National High Technology Research and Development Program of China (863 Program) (Grant No. 2012AA021003).

Author contributions

Conceptualization; ZYQ, TTL and YQH; methodology; software; ZYQ, TTL and YQH; investigation; resources; YQH, ZYQ and JHZ; validation; formal analysis; data curation; writing-original draft preparation; writing-review and editing; YQH, TTL, XYJ and ZYQ; visualization; YQH and JG; supervision; project administration; ZYQ and JHZ. YQH and TTL confirm the authenticity of all the raw data. All authors have read and agreed to the published version of the manuscript.

Data availability

The datasets generated and analyzed during the current study are available in The Cancer Genome Atlas (TCGA) repository (http://xena.ucsc.edu/), and GSE41998, GSE76540, and GSE104050 from Gene Expression Omnibus (GEO) repository (https://www.ncbi.nlm.nih.gov/geo/). Access to both repositories is not required accession number. The original contributions presented in this study are included in the article/supplementary material. Further inquiries can be directed to the corresponding author.

Declarations

Ethical approval statement

Not applicable.

Conflict of Interest Statement

The authors declare that they have no conflict of interest.

References

1 Bray, F. *et al.* Global cancer statistics 2022: GLOBOCAN estimates of incidence and mortality worldwide for 36 cancers in 185 countries. *CA Cancer J Clin* **74**, 229-263, doi:10.3322/caac.21834 (2024).

2 Gradishar, W. J. *et al.* Breast Cancer, Version 3.2024, NCCN Clinical Practice Guidelines in Oncology. *J Natl Compr Canc Netw* **22**, 331-357, doi:10.6004/jnccn.2024.0035 (2024).

3 Xiong, X. *et al.* Breast cancer: pathogenesis and treatments. *Signal Transduct Target Ther* **10**, 49, doi:10.1038/s41392-024-02108-4 (2025).

4 Desgres, M. *et al.* Resistance to neoadjuvant chemotherapy in breast cancers: a metabolic perspective. *J Exp Clin Cancer Res* **44**, 234, doi:10.1186/s13046-025-03500-w (2025).

5 Karami Fath, M. *et al.* The role of epigenetic modifications in drug resistance and treatment of breast cancer. *Cell Mol Biol Lett* **27**, 52, doi:10.1186/s11658-022-00344-6 (2022).

6 Liang, T. *et al.* Targeting histone deacetylases for cancer therapy: Trends and challenges. *Acta Pharm Sin B* **13**, 2425-2463, doi:10.1016/j.apsb.2023.02.007 (2023).

7 Park, S. Y. *et al.* Histone deacetylases 1, 6 and 8 are critical for invasion in breast cancer. *Oncol Rep* **25**, 1677-1681, doi:10.3892/or.2011.1236 (2011).

8 Sirous, H., Campiani, G., Calderone, V. & Brogi, S. Discovery of novel hit compounds as potential HDAC1 inhibitors: The case of ligand- and structure-based virtual screening. *Comput Biol Med* **137**, 104808, doi:10.1016/j.compbiomed.2021.104808 (2021).

9 Sixto-López, Y. *et al.* Hydroxamic acid derivatives as HDAC1, HDAC6 and HDAC8 inhibitors with antiproliferative activity in cancer cell lines. *Sci Rep* **10**, 10462, doi:10.1038/s41598-020-67112-4 (2020).

10 Wang, Z., Jing, X., Li, F., Chen, Y. & Huang, C. miR-3614-3p suppresses cell aggressiveness of human breast cancer by targeting AKT3 and HDAC1 expression. *Transl Cancer Res* **11**, 1565-1575, doi:10.21037/tcr-21-2419 (2022).

11 Weichert, W. HDAC expression and clinical prognosis in human malignancies. *Cancer Lett* **280**, 168-176, doi:10.1016/j.canlet.2008.10.047 (2009).

12 Bahl, S. *et al.* EGFR phosphorylates HDAC1 to regulate its expression and anti-apoptotic function. *Cell Death Dis* **12**, 469, doi:10.1038/s41419-021-03697-6 (2021).

13 Liu, X. *et al.* A Novel Class I HDAC Inhibitor, AW01178, Inhibits Epithelial-Mesenchymal Transition and Metastasis of Breast Cancer. *Int J Mol Sci* **25**, doi:10.3390/ijms25137234 (2024).

14 Miller, K. M. *et al.* Human HDAC1 and HDAC2 function in the DNA-damage response to promote DNA nonhomologous end-joining. *Nat Struct Mol Biol* **17**, 1144-1151, doi:10.1038/nsmb.1899 (2010).

15 Sakamoto, T. *et al.* A Histone Deacetylase Inhibitor Suppresses Epithelial-Mesenchymal Transition and Attenuates Chemoresistance in Biliary Tract Cancer. *PLoS One* **11**, e0145985, doi:10.1371/journal.pone.0145985 (2016).

16 Marvalim, C., Datta, A. & Lee, S. C. Role of p53 in breast cancer progression: An insight into p53 targeted therapy. *Theranostics* **13**, 1421-1442, doi:10.7150/thno.81847 (2023).

17 Berge, E. O. *et al.* Identification and characterization of retinoblastoma gene mutations disturbing apoptosis in human breast cancers. *Mol Cancer* **9**, 173, doi:10.1186/1476-4598-9-173 (2010).

18 Shi, M. Q. *et al.* Advances in targeting histone deacetylase for treatment of solid tumors. *J Hematol Oncol* **17**, 37, doi:10.1186/s13045-024-01551-8 (2024).

19 Parveen, R., Harihar, D. & Chatterji, B. P. Recent histone deacetylase inhibitors in cancer therapy. *Cancer* **129**, 3372-3380, doi:10.1002/cncr.34974 (2023).
20 Mehrpouri, M., Pourbagheri-Sigaroodi, A. & Bashash, D. The contributory roles of histone deacetylases (HDACs) in hematopoiesis regulation and possibilities for pharmacologic interventions in hematologic malignancies. *Int Immunopharmacol* **100**, 108114, doi:10.1016/j.intimp.2021.108114 (2021).
21 Minisini, M., Mascaro, M. & Brancolini, C. HDAC-driven mechanisms in anticancer resistance: epigenetics and beyond. *Cancer Drug Resist* **7**, 46, doi:10.20517/cdr.2024.103 (2024).
22 Chandrashekar, D. S. *et al.* UALCAN: An update to the integrated cancer data analysis platform. *Neoplasia* **25**, 18-27, doi:10.1016/j.neo.2022.01.001 (2022).
23 Weinstein, J. N. *et al.* The Cancer Genome Atlas Pan-Cancer analysis project. *Nat Genet* **45**, 1113-1120, doi:10.1038/ng.2764 (2013).
24 Kong, D. *et al.* The different regulatory effects of p53 status on multidrug resistance are determined by autophagy in ovarian cancer cells. *Biomed Pharmacother* **66**, 271-278, doi:10.1016/j.biopha.2011.12.002 (2012).
25 Li, J., Chen, W., Zhang, P. & Li, N. Topoisomerase II trapping agent teniposide induces apoptosis and G2/M or S phase arrest of oral squamous cell carcinoma. *World J Surg Oncol* **4**, 41, doi:10.1186/1477-7819-4-41 (2006).
26 Szklarczyk, D. *et al.* The STRING database in 2023: protein-protein association networks and functional enrichment analyses for any sequenced genome of interest. *Nucleic Acids Res* **51**, D638-d646, doi:10.1093/nar/gkac1000 (2023).
27 Li, T. *et al.* TIMER2.0 for analysis of tumor-infiltrating immune cells. *Nucleic Acids Res* **48**, W509-w514, doi:10.1093/nar/gkaa407 (2020).
28 Kim, A. *et al.* Epigenetic Regulation in Breast Cancer: Insights on Epidrugs. *Epigenomes* **7**, doi:10.3390/epigenomes7010006 (2023).
29 Wang, Y. F. *et al.* G9a regulates breast cancer growth by modulating iron homeostasis through the repression of ferroxidase hephaestin. *Nat Commun* **8**, 274, doi:10.1038/s41467-017-00350-9 (2017).
30 Tang, Z. *et al.* HDAC1 triggers the proliferation and migration of breast cancer cells via upregulation of interleukin-8. *Biol Chem* **398**, 1347-1356, doi:10.1515/hsz-2017-0155 (2017).
31 Xie, J., Liu, R., Cai, Y. & Liu, D. HDAC1: a promising target for cancer treatment: insights from a thorough analysis of tumor functions. *Transl Cancer Res* **13**, 5300-5315, doi:10.21037/tcr-24-23 (2024).
32 Krusche, C. A. *et al.* Histone deacetylase-1 and -3 protein expression in human breast cancer: a tissue microarray analysis. *Breast Cancer Res Treat* **90**, 15-23, doi:10.1007/s10549-004-1668-2 (2005).
33 Li, G., Tian, Y. & Zhu, W. G. The Roles of Histone Deacetylases and Their Inhibitors in Cancer Therapy. *Front Cell Dev Biol* **8**, 576946, doi:10.3389/fcell.2020.576946 (2020).
34 Verza, F. A., Das, U., Fachin, A. L., Dimmock, J. R. & Marins, M. Roles of Histone Deacetylases and Inhibitors in Anticancer Therapy. *Cancers (Basel)* **12**, doi:10.3390/cancers12061664 (2020).

35 Yin, Y. *et al.* The HDAC inhibitor HFY-4A improves TUSC2 transcription to induce immunogenic cell death in breast cancer. *Toxicol Appl Pharmacol* **478**, 116698, doi:10.1016/j.taap.2023.116698 (2023).
36 Lønning, P. E. & Knappskog, S. Mapping genetic alterations causing chemoresistance in cancer: identifying the roads by tracking the drivers. *Oncogene* **32**, 5315-5330, doi:10.1038/onc.2013.48 (2013).
37 Nagarajan, S. *et al.* ARID1A influences HDAC1/BRD4 activity, intrinsic proliferative capacity and breast cancer treatment response. *Nat Genet* **52**, 187-197, doi:10.1038/s41588-019-0541-5 (2020).
38 Sukocheva, O. A. *et al.* The crucial role of epigenetic regulation in breast cancer anti-estrogen resistance: Current findings and future perspectives. *Semin Cancer Biol* **82**, 35-59, doi:10.1016/j.semcancer.2020.12.004 (2022).
39 Wei, H. *et al.* Targeting redox-sensitive MBD2-NuRD condensate in cancer cells. *Nat Cell Biol* **27**, 801-816, doi:10.1038/s41556-025-01657-2 (2025).
40 Zhang, Y. *et al.* Collateral lethality between HDAC1 and HDAC2 exploits cancer-specific NuRD complex vulnerabilities. *Nat Struct Mol Biol* **30**, 1160-1171, doi:10.1038/s41594-023-01041-4 (2023).
41 Wang, D. *et al.* MBD2 regulates the progression and chemoresistance of cholangiocarcinoma through interaction with WDR5. *J Exp Clin Cancer Res* **43**, 272, doi:10.1186/s13046-024-03188-4 (2024).
42 Peinado, H., Ballestar, E., Esteller, M. & Cano, A. Snail mediates E-cadherin repression by the recruitment of the Sin3A/histone deacetylase 1 (HDAC1)/HDAC2 complex. *Mol Cell Biol* **24**, 306-319, doi:10.1128/mcb.24.1.306-319.2004 (2004).
43 Sundararajan, V. *et al.* SNAI1 recruits HDAC1 to suppress SNAI2 transcription during epithelial to mesenchymal transition. *Sci Rep* **9**, 8295, doi:10.1038/s41598-019-44826-8 (2019).
44 Fan, C. *et al.* Identification of a SNAI1 enhancer RNA that drives cancer cell plasticity. *Nat Commun* **16**, 2890, doi:10.1038/s41467-025-58032-w (2025).
45 Chen, X. *et al.* The CtIP-CtBP1/2-HDAC1-AP1 transcriptional complex is required for the transrepression of DNA damage modulators in the pathogenesis of osteosarcoma. *Transl Oncol* **21**, 101429, doi:10.1016/j.tranon.2022.101429 (2022).
46 Birts, C. N. *et al.* Expression of CtBP family protein isoforms in breast cancer and their role in chemoresistance. *Biol Cell* **103**, 1-19, doi:10.1042/bc20100067 (2010).
47 Deng, Y., Guo, W., Xu, N., Li, F. & Li, J. CtBP1 transactivates RAD51 and confers cisplatin resistance to breast cancer cells. *Mol Carcinog* **59**, 512-519, doi:10.1002/mc.23175 (2020).
48 Raza, U. *et al.* The miR-644a/CTBP1/p53 axis suppresses drug resistance by simultaneous inhibition of cell survival and epithelial-mesenchymal transition in breast cancer. *Oncotarget* **7**, 49859-49877, doi:10.18632/oncotarget.10489 (2016).
49 Gronkowska, K. & Robaszkiewicz, A. Genetic dysregulation of EP300 in cancers in light of cancer epigenome control - targeting of p300-proficient and -deficient cancers. *Mol Ther Oncol* **32**, 200871, doi:10.1016/j.omton.2024.200871 (2024).
50 Asaduzzaman, M. *et al.* Tumour suppressor EP300, a modulator of paclitaxel resistance and stemness, is downregulated in metaplastic breast

cancer. *Breast Cancer Res Treat* **163**, 461-474, doi:10.1007/s10549-017-4202-z (2017).
51 Aubrey, B. J., Kelly, G. L., Janic, A., Herold, M. J. & Strasser, A. How does p53 induce apoptosis and how does this relate to p53-mediated tumour suppression? *Cell Death Differ* **25**, 104-113, doi:10.1038/cdd.2017.169 (2018).
52 Garcia de Herreros, M. *et al.* Corrigendum to "Prognostic Expression Signature of RB1, PTEN, and TP53 Genes in Patients with Metastatic Hormone-sensitive Prostate Cancer Treated with Androgen Receptor Pathway Inhibitors" [Eur. Urol. Open Sci. 70 (2024) 86-90]. *Eur Urol Open Sci* **77**, 31, doi:10.1016/j.euros.2025.05.010 (2025).
53 Li, Z., Jia, X., Meliala, I. T. S., Li, Y. & Kasim, V. Yin Yang 1 (YY1) as a Central Node in Drug Resistance Pathways: Potential for Combination Strategies in Cancer Therapy. *Biomolecules* **15**, doi:10.3390/biom15081069 (2025).
54 Zhao, S., Allis, C. D. & Wang, G. G. The language of chromatin modification in human cancers. *Nat Rev Cancer* **21**, 413-430, doi:10.1038/s41568-021-00357-x (2021).
55 Mirzaei, S. *et al.* Nrf2 signaling pathway in cisplatin chemotherapy: Potential involvement in organ protection and chemoresistance. *Pharmacol Res* **167**, 105575, doi:10.1016/j.phrs.2021.105575 (2021).
56 Syu, J. P., Chi, J. T. & Kung, H. N. Nrf2 is the key to chemotherapy resistance in MCF7 breast cancer cells under hypoxia. *Oncotarget* **7**, 14659-14672, doi:10.18632/oncotarget.7406 (2016).
57 Ghareghomi, S., Habibi-Rezaei, M., Arese, M., Saso, L. & Moosavi-Movahedi, A. A. Nrf2 Modulation in Breast Cancer. *Biomedicines* **10**, doi:10.3390/biomedicines10102668 (2022).
58 Pang, Y. *et al.* The combination of the HDAC1 inhibitor SAHA and doxorubicin has synergic efficacy in triple negative breast cancer in vivo. *Pharmacol Res* **196**, 106926, doi:10.1016/j.phrs.2023.106926 (2023).
59 Liu, H., Zhao, H., Zhou, M., Zhao, X. & Lu, Y. Neutrophils in cancer drug resistance: Roles and therapeutic opportunities. *Cancer Lett* **611**, 217417, doi:10.1016/j.canlet.2024.217417 (2024).
60 Zeng, W. *et al.* Ferroptotic Neutrophils Induce Immunosuppression and Chemoresistance in Breast Cancer. *Cancer Res* **85**, 477-496, doi:10.1158/0008-5472.Can-24-1941 (2025).
61 Ou, B. *et al.* Senescent neutrophils-derived exosomal piRNA-17560 promotes chemoresistance and EMT of breast cancer via FTO-mediated m6A demethylation. *Cell Death Dis* **13**, 905, doi:10.1038/s41419-022-05317-3 (2022).
62 Hsu, Y. L. *et al.* Benzyl butyl phthalate increases the chemoresistance to doxorubicin/cyclophosphamide by increasing breast cancer-associated dendritic cell-derived CXCL1/GROα and S100A8/A9. *Oncol Rep* **34**, 2889-2900, doi:10.3892/or.2015.4307 (2015).
63 Ellmeier, W. Molecular control of CD4(+) T cell lineage plasticity and integrity. *Int Immunopharmacol* **28**, 813-817, doi:10.1016/j.intimp.2015.03.050 (2015).
64 Govers, A. *et al.* Transcriptomic and Epigenomic Profiling of Histone Deacetylase Inhibitor Treatment Reveals Distinct Gene Regulation Profiles

Leading to Impaired Neutrophil Development. *Hemasphere* **3**, e270, doi:10.1097/hs9.0000000000000270 (2019).
65 Mao, C. *et al.* Discovery of the First-in-Class Dual-Target ROCK/HDAC Inhibitor with Potent Antitumor Efficacy in Vivo That Trigger Antitumor Immunity. *J Med Chem* **67**, 20619-20638, doi:10.1021/acs.jmedchem.4c02183 (2024).
66 Black, M. *et al.* Activation of the PD-1/PD-L1 immune checkpoint confers tumor cell chemoresistance associated with increased metastasis. *Oncotarget* **7**, 10557-10567, doi:10.18632/oncotarget.7235 (2016).
67 Dastmalchi, N. *et al.* Molecular mechanisms of breast cancer chemoresistance by immune checkpoints. *Life Sci* **263**, 118604, doi:10.1016/j.lfs.2020.118604 (2020).
68 Berger, K. N. & Pu, J. J. PD-1 pathway and its clinical application: A 20year journey after discovery of the complete human PD-1 gene. *Gene* **638**, 20-25, doi:10.1016/j.gene.2017.09.050 (2018).
69 Cha, J. H., Chan, L. C., Li, C. W., Hsu, J. L. & Hung, M. C. Mechanisms Controlling PD-L1 Expression in Cancer. *Mol Cell* **76**, 359-370, doi:10.1016/j.molcel.2019.09.030 (2019).
70 He, X. & Xu, C. Immune checkpoint signaling and cancer immunotherapy. *Cell Res* **30**, 660-669, doi:10.1038/s41422-020-0343-4 (2020).
71 Nakhjavani, M. & Shigdar, S. Future of PD-1/PD-L1 axis modulation for the treatment of triple-negative breast cancer. *Pharmacol Res* **175**, 106019, doi:10.1016/j.phrs.2021.106019 (2022).
72 Li, Q. *et al.* The anti-PD-L1/CTLA-4 bispecific antibody KN046 in combination with nab-paclitaxel in first-line treatment of metastatic triple-negative breast cancer: a multicenter phase II trial. *Nat Commun* **15**, 1015, doi:10.1038/s41467-024-45160-y (2024).
73 Jin, M. *et al.* PD-1/PD-L1 immune checkpoint blockade in breast cancer: research insights and sensitization strategies. *Mol Cancer* **23**, 266, doi:10.1186/s12943-024-02176-8 (2024).

Figures

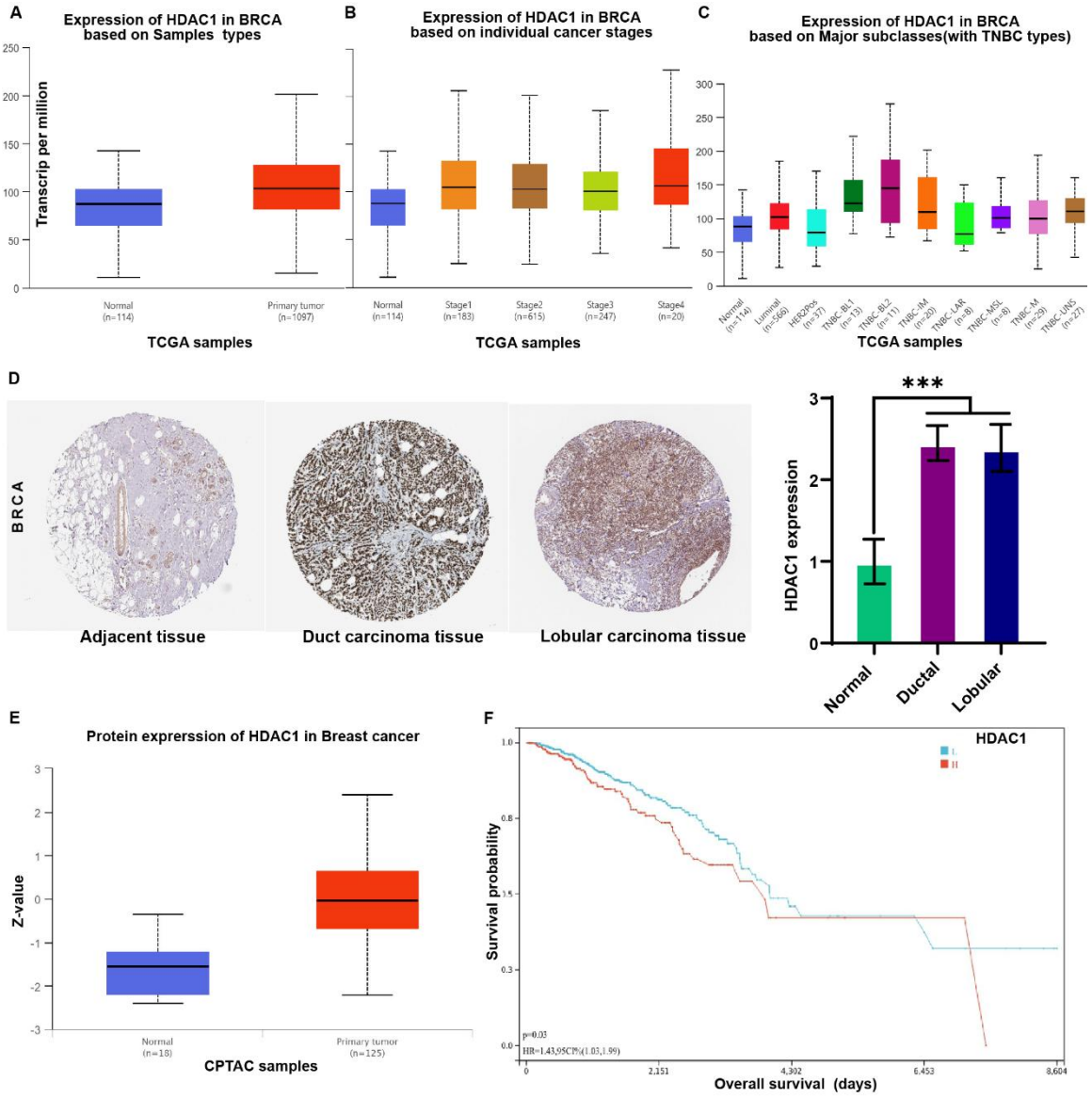
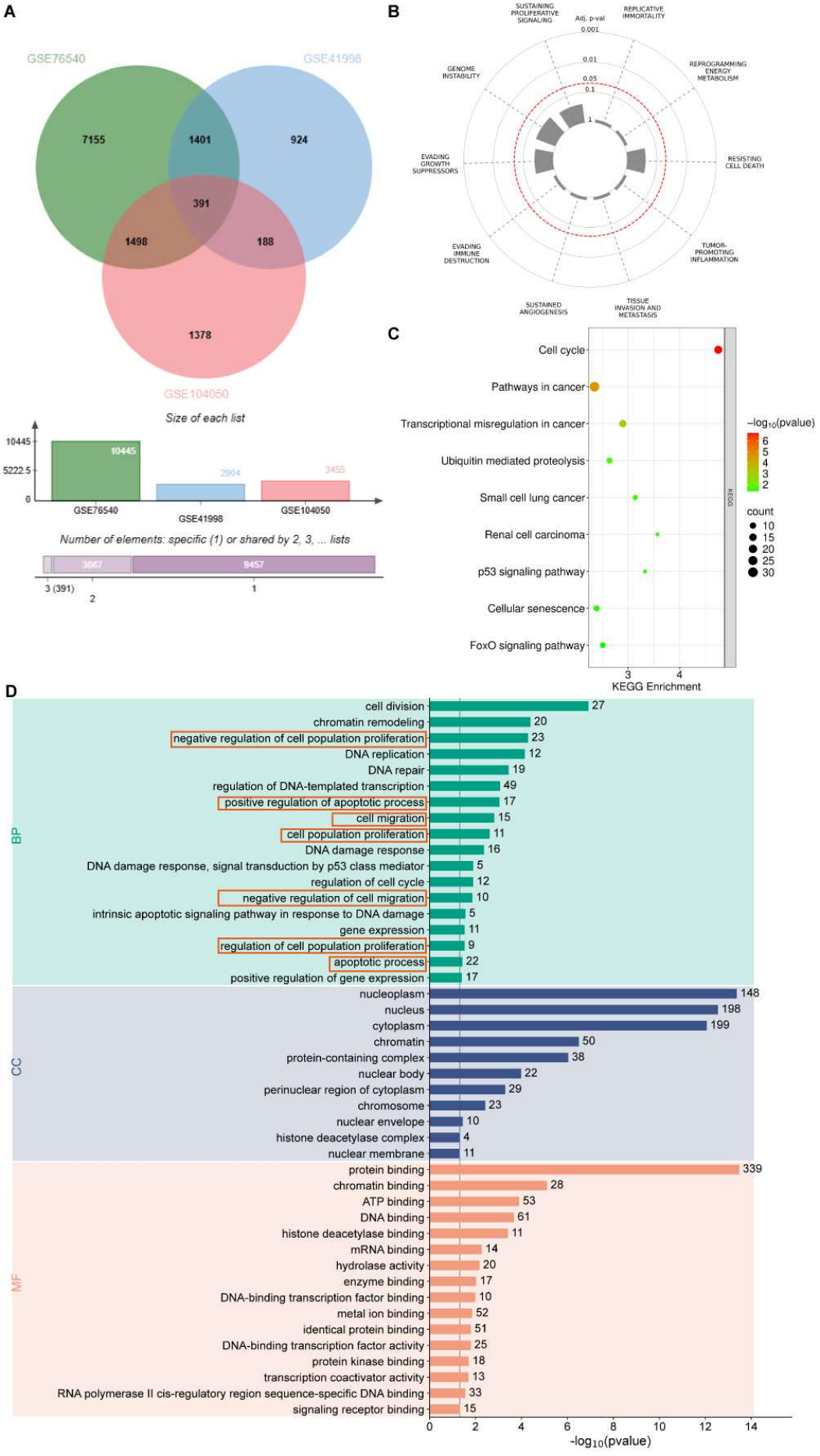


Figure 1. HDAC1 expression is significantly upregulated in breast cancer, particularly in subtypes characterized by more aggressive biological features.

(A) HDAC1 mRNA expression in primary breast cancer (BRCA) (n=1097) and normal tissues (n=114) based on TCGA dataset. Blue and red boxes represent normal and tumor groups, respectively. **(B)** HDAC1 expression across pathological stages (I–IV) in BRCA (n=183, 615, 247, and 20, respectively) compared with normal tissues (n=114) **(C)** HDAC1 expression across major subclasses of BRCA, including Luminal (n=566), HER2-positive (n=37), and TNBC subtypes (TNBC-BL1 (n=13), TNBC-BL2 (n=11), TNBC-IM (n=20), TNBC-M (n=8), TNBC-MSL(n=8), TNBC-LAR(n=29), TNBC-UNS(n=27)) and normal (n=114) tissues. **(D)** Immunohistochemical staining of HDAC1 protein in breast adjacent normal tissue, ductal carcinoma, and lobular carcinoma (HPA database). (***P<0.001 vs adjacent normal tissue). **(E)** Protein expression levels (Z-

928 scores) of HDAC1 in primary BRCA (n=125) and normal tissues (n=18) from CPTAC.
929 Z-values represent standard deviations from the median across samples for the given
930 cancer type. **(F)** Kaplan–Meier analysis of OS between high and low HDAC1 expression
931 groups in BRCA patients based on TCGA datasets. (log-rank p=0.031; HR=1.43, 95%
932 CI: 1.03–1.99).


A
GSE76540
GSE41998
GSE104050
7155
1401
924
391
1498
188
1378
Size of each list
10445
5222.5
0
10445
2904
3455
GSE76540
GSE41998
GSE104050
Number of elements: specific (1) or shared by 2, 3, ... lists
3867
9457
3 (391)
2
1
B
SUSTAINING PROLIFERATIVE SIGNALING
Adj. p-val
REPLICATIVE IMMORTALITY
0.001
0.01
0.05
0.1
1
GENOME INSTABILITY
REPROGRAMMING ENERGY METABOLISM
EVADING GROWTH SUPPRESSORS
RESISTING CELL DEATH
EVADING IMMUNE DESTRUCTION
TUMOR-PROMOTING INFLAMMATION
SUSTAINED ANGIOGENESIS
TISSUE INVASION AND METASTASIS
C
Cell cycle
Pathways in cancer
Transcriptional misregulation in cancer
Ubiquitin mediated proteolysis
Small cell lung cancer
Renal cell carcinoma
p53 signaling pathway
Cellular senescence
FoxO signaling pathway
KEGG
3
4
KEGG Enrichment
−log10(pvalue)
6
5
4
3
2
count
10
15
20
25
30
D
BP
cell division 27
chromatin remodeling 20
negative regulation of cell population proliferation 23
DNA replication 12
DNA repair 19
regulation of DNA-templated transcription 49
positive regulation of apoptotic process 17
cell migration 15
cell population proliferation 11
DNA damage response 16
DNA damage response, signal transduction by p53 class mediator 5
regulation of cell cycle 12
negative regulation of cell migration 10
intrinsic apoptotic signaling pathway in response to DNA damage 5
gene expression 11
regulation of cell population proliferation 9
apoptotic process 22
positive regulation of gene expression 17
CC
nucleoplasm 148
nucleus 198
cytoplasm 199
chromatin 50
protein-containing complex 38
nuclear body 22
perinuclear region of cytoplasm 29
chromosome 23
nuclear envelope 10
histone deacetylase complex 4
nuclear membrane 11
MF
protein binding 339
chromatin binding 28
ATP binding 53
DNA binding 61
histone deacetylase binding 11
mRNA binding 14
hydrolase activity 20
enzyme binding 17
DNA-binding transcription factor binding 10
metal ion binding 52
identical protein binding 51
DNA-binding transcription factor activity 25
protein kinase binding 18
transcription coactivator activity 13
RNA polymerase II cis-regulatory region sequence-specific DNA binding 33
signaling receptor binding 15
0
2
4
6
8
10
12
14
-log10(pvalue)

933

Figure 2. Identification and functional enrichment analysis of HDAC1 in drug resistant breast cancer.

(A) Venn diagram illustrating the intersection of three drug sensitivity-associated gene signatures from independent GEO datasets (GSE76540, GSE104050, GSE41998), screening 391 common DEGs. Bar plot shows the number of specific and shared elements across datasets. **(B)** Cancer hallmark enrichment analysis of HDAC1, with gray segments representing significantly enriched pathways (adjusted p-value < 0.05). **(C)** KEGG pathway enrichment analysis of HDAC1-associated genes in breast cancer, showing significant enrichment in multiple cancer-related pathways. (The pathway analysis was performed using the KEGG database; Kanehisa and Goto, Nucleic Acids Res, 2000.) **(D)** GO functional enrichment analysis of HDAC1 in breast cancer, showing BP, CC, and MF. Red boxes highlight key processes: apoptotic process, cell population proliferation, and cell migration.

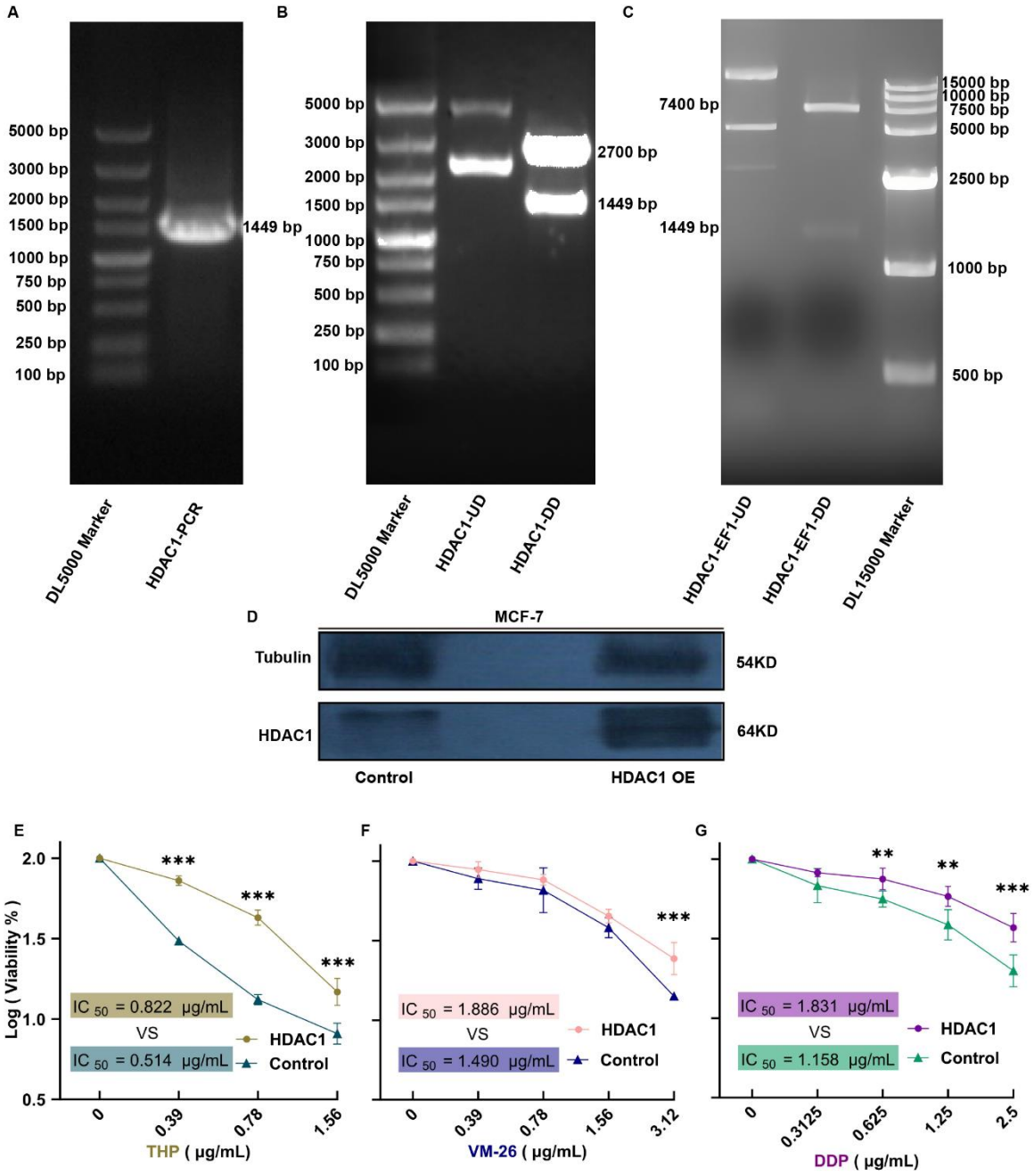


Figure 3. Lentiviral-mediated HDAC1 overexpression markedly increased the survival rate of MCF-7 cells following treatment with VM-26, DDP, and THP.

(A) Agarose gel electrophoresis of the PCR-amplified HDAC1 coding sequence showing a single specific band of the expected size (1449 bp). **(B)** Agarose gel electrophoresis of the recombinant pSIMPLE-18T–HDAC1 plasmid before (UD) and after double-enzyme digestion (DD). Double digestion released a 2700-bp vector backbone and a 1449-bp HDAC1 insert. **(C)** Agarose gel electrophoresis of the recombinant pCDH-CMV-MCS-HDAC1-EF1-Puro lentiviral vector before (UD) and after double-enzyme digestion (DD). Double digestion yielded bands of approximately 7400 bp corresponding to the

vector backbone and 1449 bp corresponding to the HDAC1 insert. **(D)** Representative Western blot showing HDAC1 protein expression in MCF-7-Control and MCF-7-HDAC1 cells, with tubulin as the loading control. **(E–G)** Dose–response curves of MCF-7-HDAC1 and MCF-7-Control cells treated with THP **(E)**, VM-26 **(F)**, and DDP **(G)**, respectively. (All **P < 0.01, ***P < 0.001 vs MCF-7-Control group).

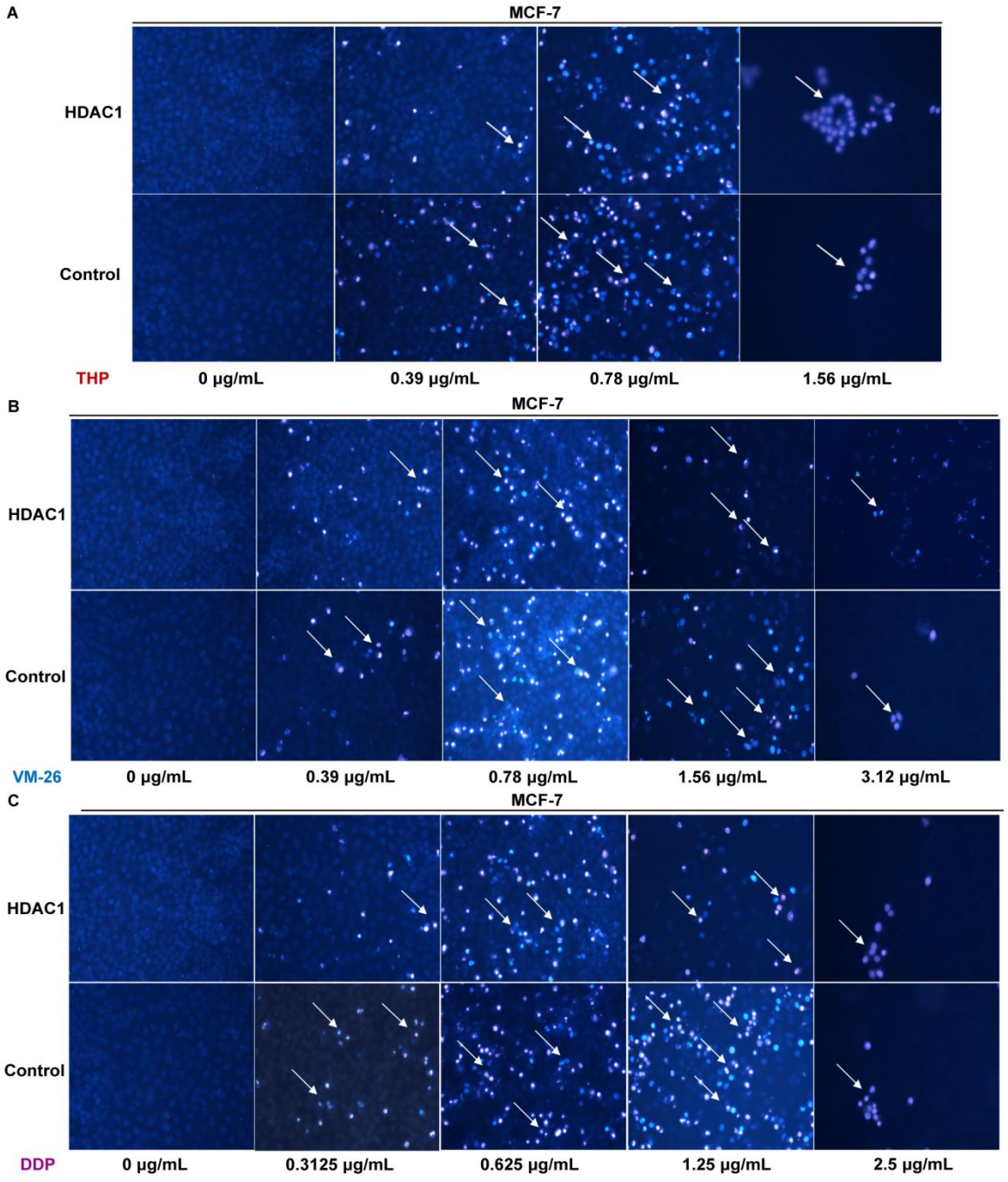


Figure 4. Lentiviral-mediated HDAC1 overexpression markedly reduced nuclear abnormalities and cell death of MCF-7 cells following treatment with VM-26, DDP, and THP.

(A–C) Hoechst33258/PI dual staining of MCF-7-HDAC1 and control cells following 72-hour exposure to (A) THP, and 48-hour exposure to (B) VM-26, and (C) DDP at the indicated concentrations. Representative images show nuclear morphology (blue fluorescence) with apoptotic features (condensed and fragmented nuclei) indicated by arrows. White arrows indicate apoptotic cells with condensed nuclei, while red arrows indicate dead cells with fragmented nuclei. All images are representative of three independent experiments.

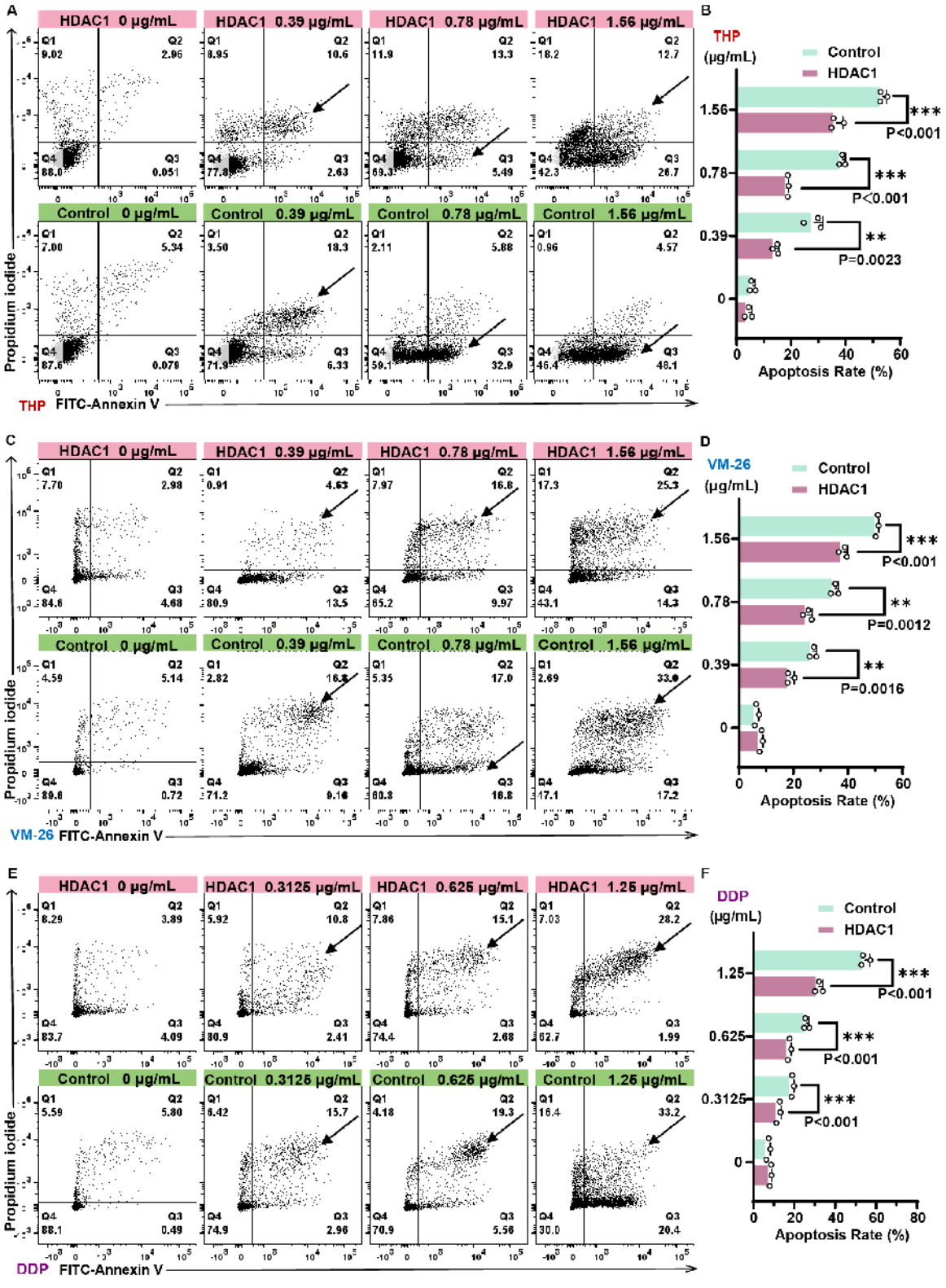


Figure 5 Lentiviral-mediated HDAC1 overexpression reduces chemosensitivity by attenuating chemotherapy-induced apoptosis in MCF-7 breast cancer cells.

(**A-C**) Representative flow cytometry plots showing apoptosis in MCF-7-HDAC1 (top) and MCF-7-Control (bottom) cells following treatment with THP for 72 h (**A**), VM-26

for 48 h (**B**), and DDP for 48 h (**C**). Apoptosis was assessed by Annexin V-FITC/PI staining and flow cytometry. (**D-F**) Quantification of the apoptotic cell population following treatment with THP (**D**), VM-26 (**E**), and DDP (**F**). (All **P < 0.01, ***P < 0.001 vs MCF-7-Control group). The total apoptotic population was calculated as the sum of Annexin V-positive/PI-negative and Annexin V-positive/PI-positive cells. Values are expressed as mean ± SD from three independent experiments.

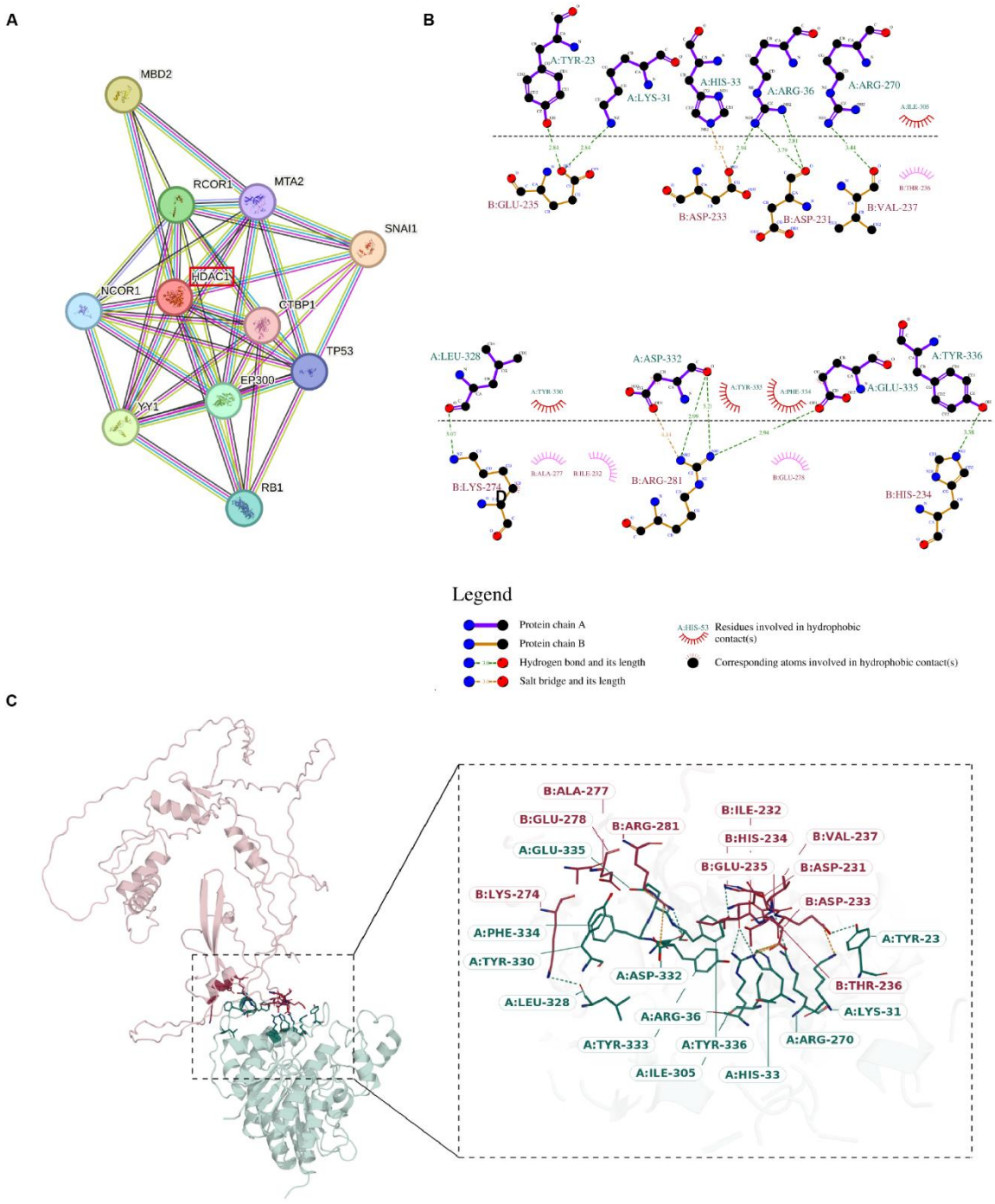


Figure 6 HDAC1-associated PPI network and structural analysis of the predicted HDAC1-YY1 interaction.

(A) PPI network of HDAC1-associated genes, node color represents gene function. **(B)** Two-dimensional LigPlot analysis of the predicted HDAC1–YY1 interaction interface, highlighting interacting residues. **(C)** Three-dimensional overall conformation of the predicted HDAC1–YY1 complex and the major intermolecular interactions at the binding interface.

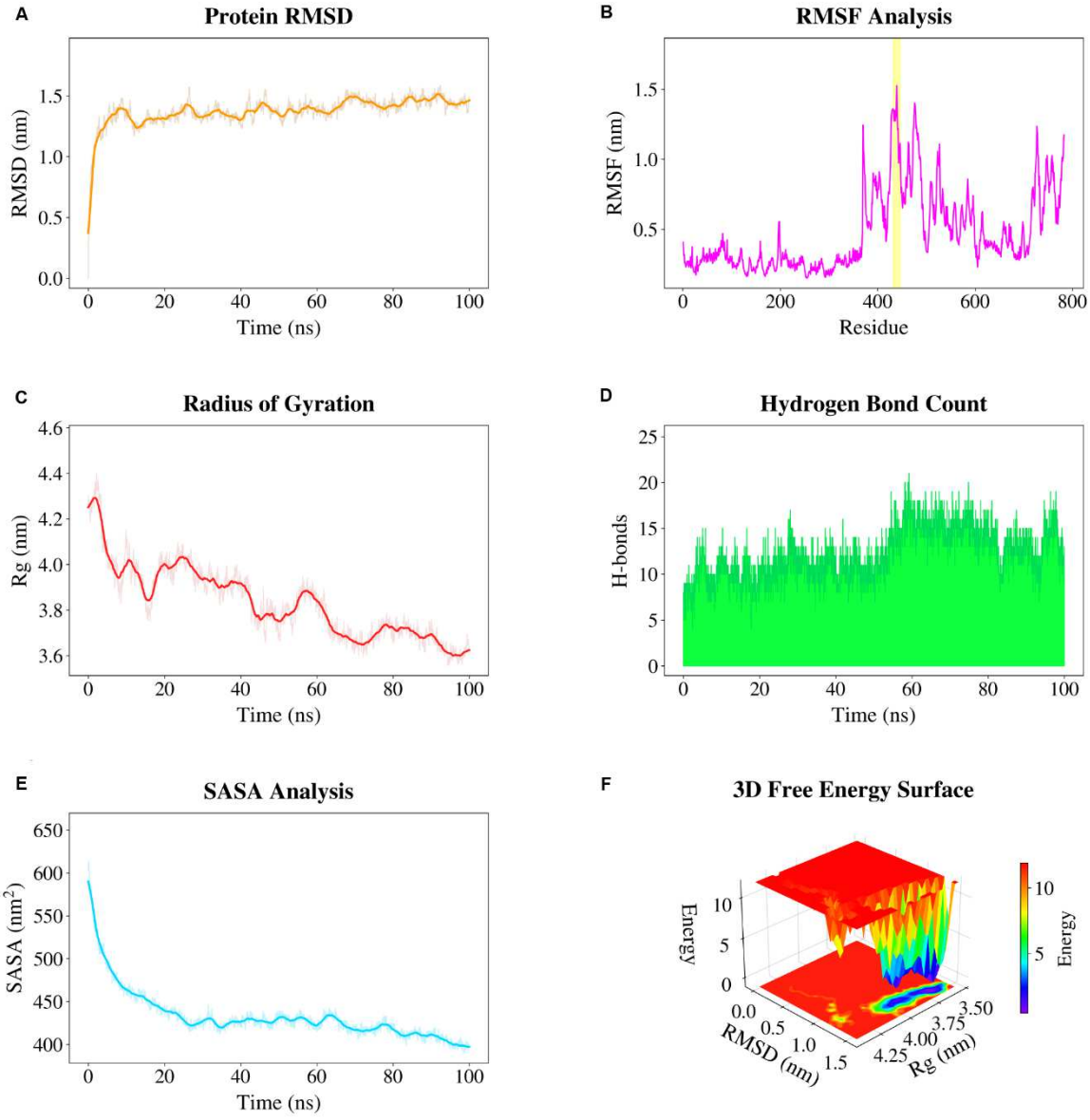


Figure 7. Structural stability and conformational dynamics of the HDAC1–YY1 complex during molecular dynamics simulation.

(A) RMSD of the HDAC1–YY1 complex over 100 ns. (B) Residue-wise RMSF, with continuous residue numbering along the x-axis for the entire system. **(C)** Radius of gyration (Rg). **(D)** Number of intermolecular hydrogen bonds at the Protein A–Protein B interface. **(E)** Solvent-accessible surface area (SASA). **(F)** Three-dimensional free-

energy landscape based on RMSD and *Rg*, showing the distribution of conformational states and the major low-energy regions.

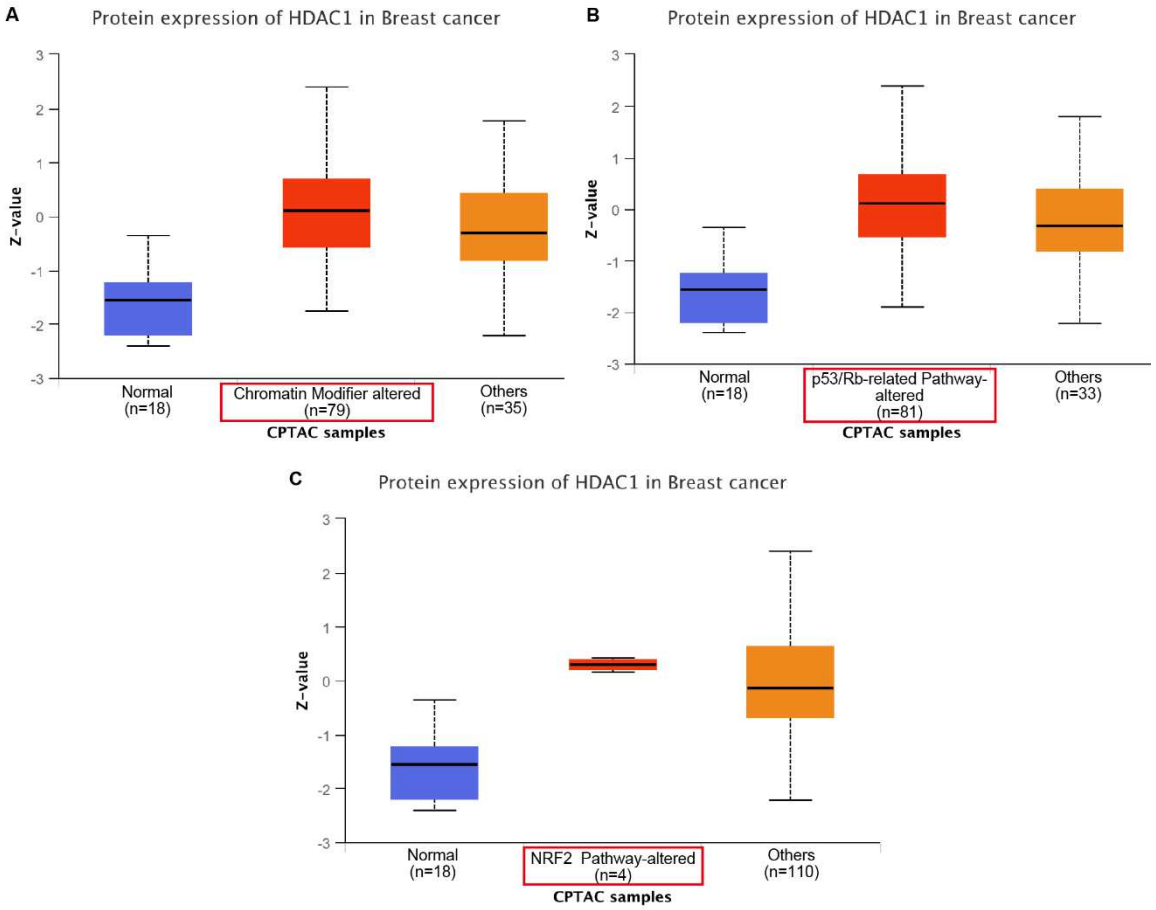


Figure 8 HDAC1 expression across chromatin-modifier, P53/RB1, and NRF2 pathway states in breast cancer.

(A-C) Comparative analysis of HDAC1 protein expression (Z-scores) in normal breast tissue(n=18) versus breast cancers with alterations in (**A**) chromatin modifiers(n=79), (**B**) p53/Rb pathway(n=81), and (**C**) NRF2 pathway(n=4). The others group includes samples with alterations in pathways other than the indicated pathway.

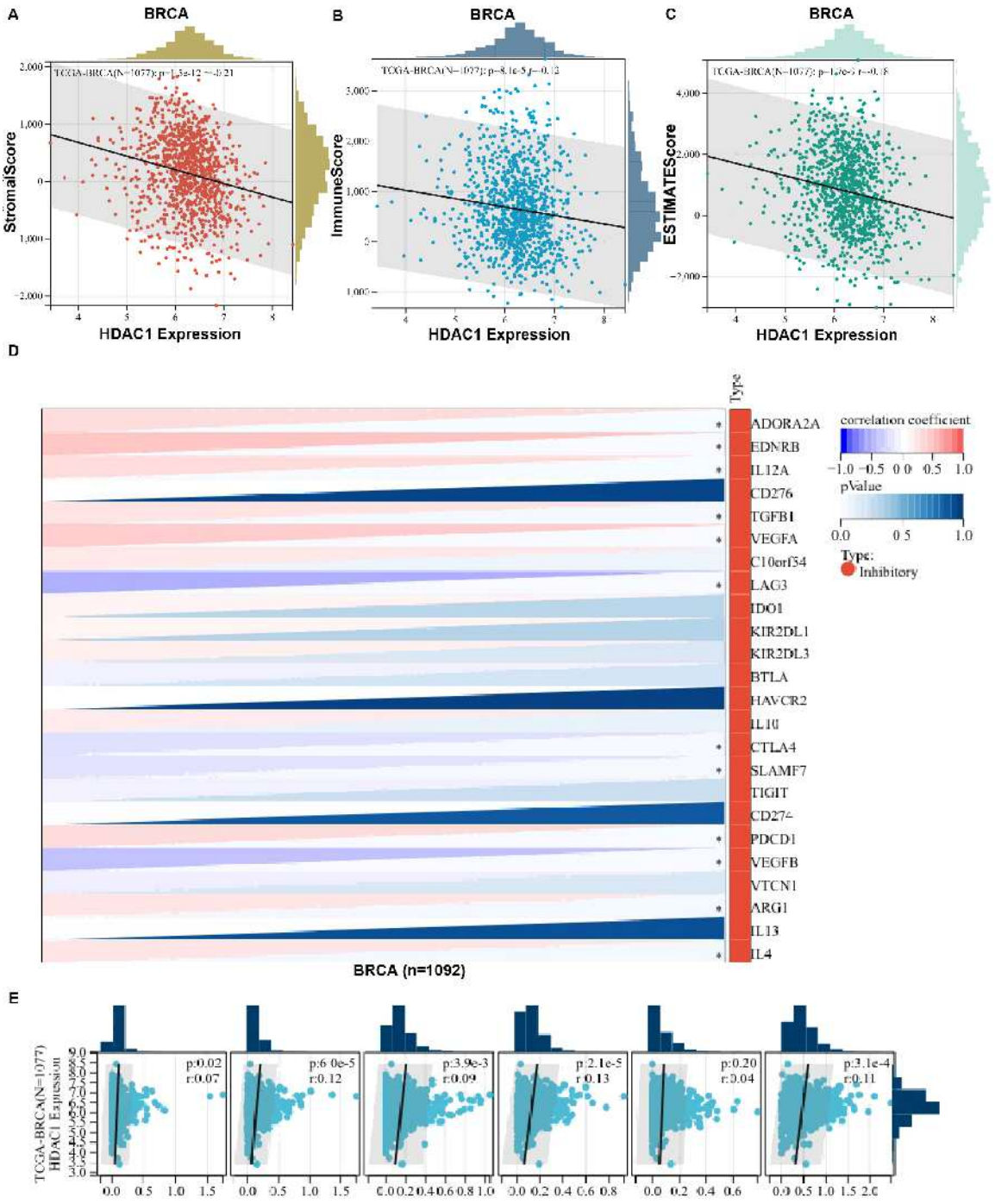


Figure 9 HDAC1 expression correlates with tumor microenvironment and immune checkpoint interactions in breast cancer.

(A–C) Scatter plots showing Pearson's correlation coefficients between HDAC1 expression and (A) stromal score, (B) immune score, and (C) ESTIMATE score in breast cancer (BRCA). Black lines represent linear regression trends; gray areas indicate 95% confidence intervals. Data were analyzed using the ESTIMATE algorithm. **(D)** Heatmap illustrating Pearson's correlation coefficients between HDAC1 and 24 inhibitory immune

checkpoint genes across breast cancer samples (TCGA datasets). Red indicates positive correlations; blue indicates negative correlations; black dots denote statistically significant associations ($p < 0.05$). **(E)** Scatter plots showing the relationship between HDAC1 expression and immune cell infiltration levels in BRCA. Each panel displays Pearson's correlation coefficient (r) and p-value for B cells, $CD4^+$ T cells, $CD8^+$ T cells, neutrophils, macrophages, and dendritic cells. Gray areas represent 95% confidence intervals. Data were analyzed using the TIMER algorithm.

Tables

Table1. List of reagents and materials

Experimental materials	Supplier/manufacturer	Lot number
DH5α competent cells	Solarbio	
MCF-7	Tumor Cell Bank at the Chinese Academy of Medical Sciences	TCHu 74
293-T	Cancer cell bank, Chinese academy of medical sciences	
pSIMPLE-18 EcoR V/BAP Vector	Takara	D105A
pCDH-CMV-MCS-EF1-Puro	Addgene	CD510B-1
pMDLg/pRRE	Addgene	12251
pRSV-Rev	Addgene	12253
pMD2.G	Addgene	12259
DMEM (high glucose)	Hyclone	AXM75422
XbaI	Takara	K3801CA
EcoRI	Takara	CK2103A
DNA Marker DL5000	Takara	A1001A
DNA Marker DL15000	Takara	A301A
HDAC 1 antibody	Cell signaling technology	2062
Tubulin antibody	Beyotime	AT819-1
HRP-conjugated secondary antibody	Zhongshan-golden bridge	970380
Supersensitive ECL chemiluminescence kit	Beyotime	107724
THP: 1 mg/mL	Shenzhen Wanle pharma	20120321
VM-26: 10 mg/mL	Beijing double-crane pharma	20111210

DDP: 5 mg/mL	Yunnan biovalley pharma	20110901
MTT	Amresco	0793
Hoechst33258	Jiancheng bio	20120224
PI	Solarbio	20120809
Annexin V/PI apoptosis detection kit	BD	556547

Table 2. GEO sample list: sensitive vs resistant groups

GEO accession	Organisms	sensitive samples	resistant samples
GSE41998	Homo sapiens	Breast cancer patients sensitive to neoadjuvant ixabepilone or paclitaxel treatment following doxorubicin/cyclophosphamide chemotherapy (n=201)	Breast cancer patients resistant to neoadjuvant ixabepilone or paclitaxel treatment following doxorubicin/cyclophosphamide chemotherapy (n=69)
GSE76540	Homo sapiens	Parental chemosensitive MCF-7 breast cancer cells (n=3)	Chemoresistant MCF-7 breast cancer cells (n=3)
GSE104050	Homo sapiens	Parental Tamoxifen-sensitive MCF-7 breast cancer cells (n=2)	Tamoxifen-resistant MCF-7 breast cancer cells (n=1)

Table3. Primer information for HDAC1

Name	Primer sequence (5'-3')	Restriction Site	Product size
HDAC 1sense	GC**TCTAGAGCCACC**ATGGCGCAGACGCAGG	XbaI	1449 bp
HDAC 1 antisense	CG**GAATTC**TCAGGCCAACTTGACCTCC	EcoRI	

Supplementary Materials

Table S1. Summary of structural stability, residue-level energy contributions, and MM-PBSA binding energy of the HDAC1–YY1 complex.

Supplementary Files

This is a list of supplementary files associated with this preprint. Click to download.

- FIGURES3.tif
- FIGURES1.tif
- FIGURES2.tif
- SupplementaryInfoFile.pdf
- FIGURES4S7.tif